HIBBARD, L. U.
National Standards Laboratory
CSIRO
Australia

Proc. Symposium on Earth's Gravitational Field & Secular Variations in Position (1973), 622-636.

THE STABILITY OF MICROWAVE FREQUENCY STANDARDS AND THEIR EFFECTS ON SECULAR VARIATION STUDIES

ABSTRACT

Atomic resonances in the microwave region are the present basis for accurate frequency, time interval and time standards. Rubidium standards are light in weight and cheap enough for any purpose requiring an accuracy of 5×10^{-10} and stability (> 100 s) of 10^{-12}. Commercial caesium beam standards are the workhorse of the frequency standard industry. Only the most stringent applications call for a better performance. Individual clocks are accurate over long periods to better than 10^{-11} and for some years past a batch of clocks has been used to maintain a continuous long term accuracy better than 10^{-12}.

The hydrogen maser is comparatively expensive and cumbersome but not excessively so for the most demanding applications calling for stability. Its accuracy (10^{-12}) approaches that of the best laboratory caesium beam standards and its stability (> 10 s) of 10^{-14} is better by more than an order of magnitude.

A revolution in technique is now in progress with the extension of electronic capabilities to terahertz regions. The stabilization of masers and lasers by atomic beams or by absorption cells gives promise of accuracies beyond 10^{-13} together with reductions in magnetic sensitivity, weight and size.

1. Introduction

For some secular variation studies accurate measurement of time interval is essential, for others stable measurement is of greater importance. At the present time, the most accurate time standards are not the most stable. The current definition of the SI second (BEEHLER ET AL 1965) is based on a caesium hyperfine resonance and there is no more accurate alternative available. Long baseline interferometry (LBI) workers, however, prefer the hydrogen maser because it is over an order of magnitude more stable. At this stage it is not as accurate but this situation could change. On the other hand both devices might be superseded by standards which may or may not be envisaged at the moment.

2. Quartz Crystal Frequency Standards

The quartz oscillator is not an absolute standard of frequency and it has serious drift and rate-of-drift effects. For times less than 0.1 s a quartz oscillator has a stability better than most atomic devices and high frequency (100 MHz) crystals are appreciably better than low frequency (5 MHz) types in this respect. For longer times, good crystals have a drift rate as low as 5×10^{-10} per day and a stability of 5×10^{-12}, the lower frequencies having the better performance.

If crystal oscillators are switched off for a period they take a long while to settle down again to their best performance and may then differ by 10^{-9} or more from the previous value. Despite these faults, they play an indispensable role with all frequency standards either passive or active. For passive standards, crystals supply a basic frequency from which the atomic excitation is synthesized. For active standards, they supply a similar synthesized frequency for comparison with the atomic oscillation. In both cases, the quartz oscillator is servo-controlled by the atomic device, but the short-term stability (< 0.1 s) is due to the quartz oscillator alone. All other frequencies and clock signals are subsequently derived from the quartz oscillator.

3. Atomic Frequency Standards

The caesium beam standard (MOCKLER 1961; GLAZE 1970) is a passive device in which a high frequency magnetic field synthesized from a relatively low frequency quartz oscillator is made to interact with a collimated beam of neutral caesium atoms and gives rise to a transverse deflection of the beam. The basic elements of such a standard are shown in figure 1. Atoms are evaporated from a narrow slit in an oven and pass through a deflecting magnet in which there is an intense magnetic field gradient. The field magnetically polarizes each atom and the field gradient acts on the resulting magnetic moments and produces sideways deflections. By this means atoms in a particular hyperfine state are separated and channelled through an interaction region and a second deflecting magnet to a detector. The hyperfine states of alkali atoms are caused by coupling of the spins of the outermost electron and the nucleus. The spins, in general, either align in the same direction or in the opposite direction. As each spin has an associated magnetic moment there is an energy due to interaction of these magnetic dipoles. Transitions between one hyperfine state and another are produced by a suitable magnetic field which resonates with the energy difference between the two states,

$$\text{i.e. } h\nu = E_1 - E_2$$

where ν is the frequency, E_1 and E_2 the energies and h is Planck's constant. Such a field applied in the interaction region changes the hyperfine state of the atoms in flight and on subsequent passage through the second magnetic deflector changes the number which reach the detector. Variations in the detector output are an indication of resonance between the atoms and the rf field and are used to servo-control the frequency of the basic quartz oscillator. The accuracy of such a standard depends on the interaction time and hence on the length of the interaction space. However, if the path is made very long, the number of atoms which can be focussed through it is reduced and the detector signal may be impaired by 'shot' noise. For this reason, a short but intense beam can be comparable with a long weaker beam as regards accuracy. Excellent commercial caesium beam standards have been made by several companies and are being used in considerable numbers; nevertheless the best laboratory standards use beam lengths of some metres. The commercial standards are designed for continuous operation but the laboratory standards to date have been used on an intermittent basis and require other continuously operating standards to be used as flywheels.

The hydrogen maser (figure 2) (RAMSEY 1965; RAMSEY 1972) uses a hexapole magnetic lens to select a beam of hydrogen atoms by focussing them through the small entrance to a quartz bulb. Unwanted atoms are defocussed and discarded. The atoms that enter the bulb take about a second to escape through the same hole and during this time interact with the field in a resonant cavity.

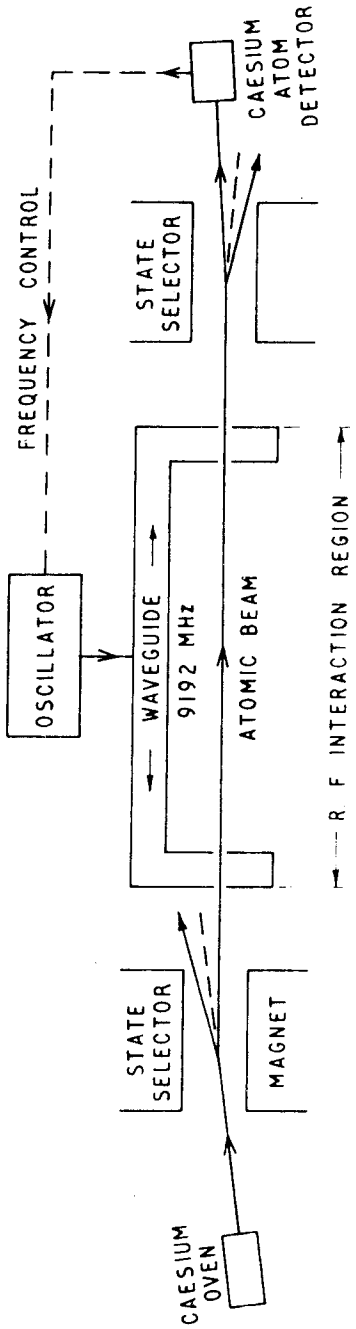

Figure 1. Caesium Beam Frequency Standard

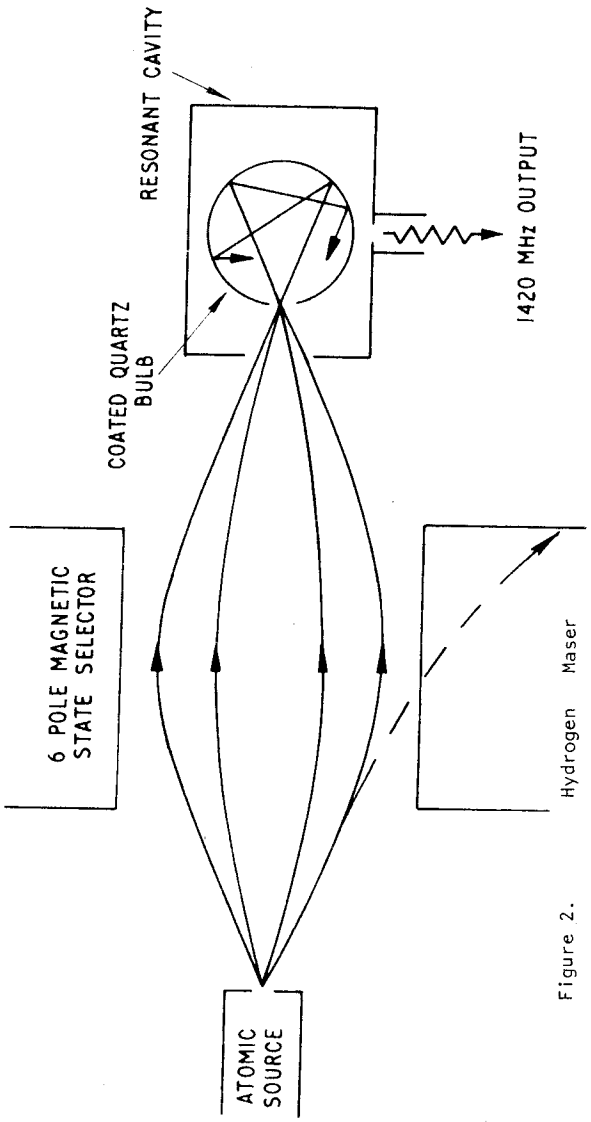

Figure 2. Hydrogen Maser

The field stimulates the atoms to change the hyperfine state and in so doing to emit energy at the hyperfine frequency of 1420 MHz. The cavity field builds up by itself and oscillates continuously without requiring an auxiliary oscillator. However it is still found necessary to servo-lock a basic quartz oscillator to the maser in order to be able to generate the clock pulses and other frequencies that are required of a standard. The maser is a continuous 'active' oscillator and achieves its superior stability because of the long interaction time, while the atoms bounce around inside the bulb. In this sense it is equivalent to a very long beam. The bulb not only confines the atoms but its temperature also determines the mean squared velocity $\overline{v^2}$ of the interacting atoms and hence a 'second-order doppler' frequency correction $\overline{v^2}/2C^2$ due to the 'time dilatation' effect of special relativity. The high stability due to containment is offset by a loss in absolute accuracy caused by phase shifts during the wall collisions. The best wall surface is Teflon and even with this there is an accumulated frequency change of about 2 parts in 10^{11} at room temperature. The uncertainties in this figure as yet prevent the full realization of the maser's capabilities.

There is not a clear cut 'best' standard. If the hydrogen maser were to receive as much development effort as has been applied to the caesium beam it may surpass it in accuracy as well as stability. This can only be decided in the future but in the meantime the same might be said of other contenders. Thallium is an attractive alternative to caesium for a beam standard; however, there are some technical problems and any ultimate advantage hardly seems to warrant the effort.

Historically the hydrogen maser grew out of attempts to make a passive beam device with a folded-up interaction path. More recently there has been advocacy (HELLWIG 1970 A) for a return from the active to the passive concept and to make the atoms emerging from the containment bulb pass through a second state selector to a detector. Another variant proposed is to couple rf power into and out of the resonant cavity and to detect the dispersion signal caused by the atoms (HELLWIG & BELL 1972). Each of these proposals has compensating disadvantages and is still left with the 'wall shift' uncertainty. The program at the CSIRO National Standards Laboratory is directed at minimizing the wall shift uncertainty of the H maser by operating at a temperature (> 80°C) at which the shift for Teflon is known to pass through zero (VESSOT ET AL 1970; ZITZEWITZ & RAMSEY 1971). The outstanding problem is to establish this temperature accurately and to be able to reestablish it whenever there is a possibility that it might have changed.

4. Frequency Stability

Frequency stability, which is identical with time-interval stability, is fashionably described in terms of the 'Allan Variance' $\sigma^2_{\Delta f/f}(2, t)$ which is equal to $\frac{1}{2}\langle(f_{n+1} - f_n)^2\rangle$ where f_n is the average frequency measured over the nth interval of time 't'. Typical plots of the square root of the 'Allan Variance' against t are shown in figure 3 for the caesium and hydrogen standards. Corresponding results for commercial rubidium standards are also included as these, together with the commercial caesium standards, are the only ones readily available off the shelf for general use. The rubidium standard uses optical pumping of rubidium vapour in a buffer gas and as a consequence is not in the category of an absolute standard. The typical drift rate is better than 10^{-11} per month but is sufficient to necessitate periodic recalibration at intervals of a year or two. Despite this low price and size make it the best choice for most applications.

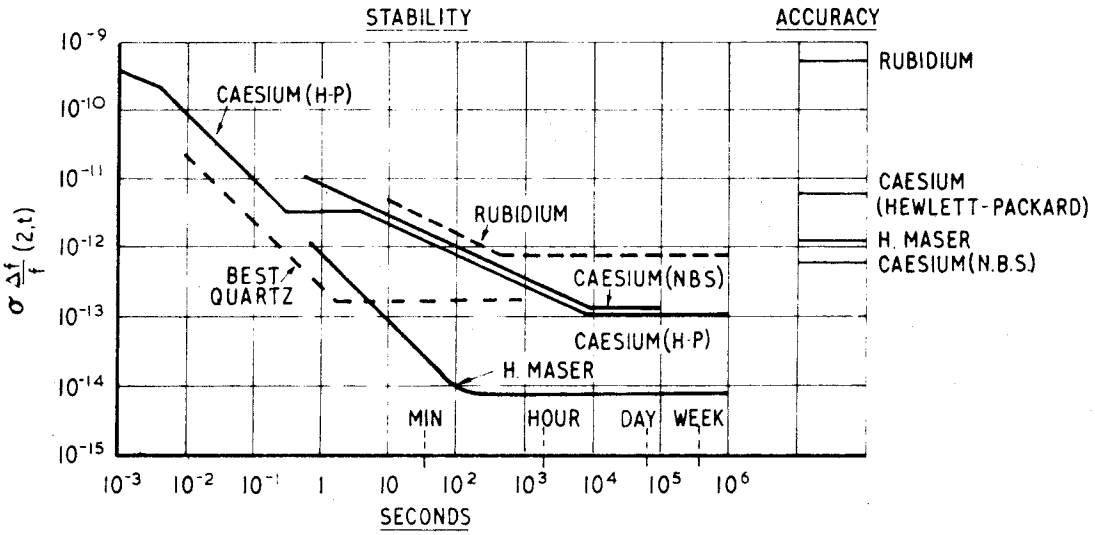

Figure 3. Frequency Stability of Atomic Standards

The long caesium beams have all been custom built by standards laboratories and have not as yet been developed for more general use. Hydrogen masers have not had as much attention for standards laboratory use but have been developed in a semi-commercial way and small numbers have been transported to remote users for LBI and space purposes. They have been most successful in applications requiring very high stability over periods of hours. They are transportable rather than portable. The smallest developed to date has a weight of some 500-600 lbs and requires 4 men to move it (LEVINE & VESSOT 1970). Transportation by plane and even by satellite is practicable. While undoubtedly expensive and complex they are not excessively so when considered in relation to the military, astronomical or space applications for which they have been developed. Already there are prospects that operating lifetimes of the order of 10 years will be achieved without major overhaul. Given skilled attention and some duplication of equipment to allow servicing, adequate continuity and indefinite high quality performance can be expected.

The frequency stability characteristics of all standards improve with time interval for intervals up to some seconds, and then level off as shown in figure 3. In general there are characteristic regions in which the stability of a standard is determined by different causes. For short times the subsidiary crystal determines the performance, and noise effects give rise to a 1/t characteristic. For longer times the stability may improve as $1/\sqrt{t}$ and a final levelling off is interpreted as 'flicker' type behaviour.

Commercial atomic standards operate continuously and typically receive no attention until a noticeable defect occurs. Their stability is often very good, approaching 10^{-13} for periods of weeks or months. However they can change abruptly in frequency and rate but should stay within their overall accuracy specification. Representative accuracy figures for the various standards are also shown in figure 3. The latest commercial caesium beam by Hewlett-Packard is specified to 7 parts in 10^{12} in accuracy. The accuracy of the best laboratory caesium standards is about 5 in 10^{13} for some hours (GLAZE 1970). To achieve indefinite long term accuracy of this order they employ a substantial number of quartz crystals and/or commercial caesium or rubidium standards to supply the continuity. High accuracy is maintained by regular and systematic evaluation of the possible errors of the caesium beam and frequent measurement of the frequencies and rates of the subsidiary standards.

The best laboratory hydrogen masers (HELLWIG ET AL 1970) require periodic reevaluation of the 'wall shift' in order to maintain accuracy to 1 in 10^{12}. Improvement to 1 in 10^{13} is forseeable with better understanding of the wall effect. The resonant cavity must be kept accurately tuned to the maser frequency and this can be done automatically or periodically. However the best stability of 1 in 10^{14} or better is only achieved when the cavity tuning is left alone. The transportable masers have not been designed for 'self' evaluation of the wall shift and the completed maser must be checked against other standards if the best accuracy is required. Despite this they are the best available standards for LBI use. For lunar ranging (LURE TEAM 1970) which requires timing accuracies of about 1 nanosecond in 2.5 seconds the rubidium standard is adequate although a commercial caesium standard would not be extravagant as it does not require recalibration.

5. Long Baseline Radio Interferometry

With the current LBI technique, beats between the incoming radio waves and a locally synthesized signal are simultaneously recorded on tape at the separate stations and cross-correlated at a later date. The computer which does the correlation can compensate for disagreements in the synthesized frequencies and the time epochs and even in the rates-of-change of frequency. It is more important for the frequencies to be stable or to drift stably over the recording period than it is for them to be known absolutely or to be in the closest agreement. Recent experiments show that time synchronization can be established retrospectively by LBI studies to within ± 1 nanosecond and that frequency differences can be measured to some parts in 10^{14} (KLEMPERER 1972). Not only do the LBI programs not suffer from current time and frequency inaccuracies but a valuable byproduct of them is an accurate method of intercontinental synchronization of epoch and frequency. The ± 1 ns accuracy of time comparison is largely set by atmospheric delays which are equivalent to a few metres of path (MATHUR ET AL 1970). Important variations are caused by water vapour and barometric pressure. The LBI and Lunar Ranging programs allow these effects to be studied in their own right and this in turn will lead to further improvement in accuracy.

It should be noted that in both the LBI and lunar ranging cases and presumably any other distance measuring situation, frequency and time interval are not the primary quantities in the measurement. The quantities that are determined are the numbers of wavelengths of the radiation under consideration. Time only enters the equations after the velocity of light is inserted. Thus the question as to whether our frequency standards remain invariable over centuries, while interesting in its own right, is not relevant to the studies under consideration.

6. World Time and Frequency

A number of countries produce standard frequency and time broadcasts that are disseminated widely. These are generated from caesium standards, either by long laboratory types or by batches of commercial units. Some claim an accuracy approaching 5 parts in 10^{13} and a number are synchronized in time to a microsecond. This has been achieved by radio, satellite and US Navy flying clock programs (RAMASASTRY ET AL 1973; WINKLER 1970), but there is as yet no accepted or regular procedure. Individual broadcasts are monitored by other centres and the results are collated by an international agency. From all of this an international standard (SMITH 1972) is derived by assigning weights to the various measured broadcast frequencies. The resultant differences between the international standard frequency and the component standards are published and corrections may be applied in retrospect as desired by these stations and by those relying on them.

'Real time' accuracy in the derivative centres can only be achieved by having a local 'flywheel' standard which is continuously compared with radio broadcasts and checked by any other means that are available. Radio propagation errors can be quite large and variable and, because of multiple path interference, ambiguities of some tens of microseconds can arise in remote parts of the globe. These can be resolved by continuously recording more than one broadcast and comparing them with locally generated standards. The local standard requires at least a couple of commercial caesium standards if the distance from a broadcast centre is large. In the northern hemisphere coordination of standards is also achieved via the Loran C networks. The 8 Loran chains comprising a total of 30 stations are synchronized to within ± 5 μs. With knowledge of the published variations an accuracy of $\pm \frac{1}{2}$ μs can be achieved (KLEMPERER 1972).

Synchronization to 0.1 μs is possible by the use of stationary satellites (RAMASASTRY ET AL 1973) but this is an inconvenient and expensive process as it requires simultaneous two way transmissions of timing signals and suitably positioned stations. Two clocks differing by 1 in 10^{12} will drift apart by 0.1 μs in a day. Thus weekly synchronization is desirable if 1 μs timing accuracy is to be maintained. This is a strong argument for improving clock stability beyond the present limits. Stability is more important than accuracy in this respect as coordination of time is becoming more necessary every day, whereas accuracy of time scale and frequency are more than adequate for all known requirements.

7. Aircraft Collision Avoidance

The most promising method of aircraft collision avoidance is one based on the simultaneous emission of radio pulses from every aircraft (BRENNAN 1971). For this to be effective the aircraft clocks must be synchronized with ground stations over substantial areas. A proposed specification for synchronism of individual ground stations for this purpose already calls for a timing accuracy of 60 ns. The more densely populated areas of the northern hemisphere can be expected to move towards a system of time coordination approaching this accuracy and a comparable global system is likely in the foreseeable future. In addition to the substantial technical problems of improving clock stability, accuracy and coordination over large areas the requirements for widespread nanosecond intelligence raise to a practical everyday level some hitherto academic aspects of relativity.

8. Relativistic Time and Frequency Corrections

The experiment by HAFELE in 1971 has conclusively resolved any doubts concerning both the clock paradox and the variation of clock rate with gravitational potential (HAFELE 1972).

By flying a batch of four caesium clocks round the world as quickly as possible on commerical airlines he eliminated from both corrections any considerations of light propagation, doppler shift, change of photon energy and frequency etc. The results clearly demonstrate that moving a clock around the earth in the direction of rotation slows the clock compared with a clock that is stationary on the earth, and one proceeding in the opposite direction speeds up. The effect of the earth's gravitational field was likewise evaluated and good agreement was obtained. Both effects are in agreement with general relativity, although the first effect can be 'derived' from the restricted principle. The expression for a clock moving eastward at the equator with velocity v and height h relative to the ground is (HAFELE 1972)

$$\frac{\Delta t}{t_o} = \frac{t - t_o}{t_o} = \frac{gh}{c^2} - \frac{2R\Omega v + v^2}{2c^2}$$

t is the time recorded by the flying clock,
t_o is the time recorded by a clock on the earth's surface,
R is the radius of the earth,
Ω is the angular velocity of the earth,
g is the acceleration due to gravity at the earth's surface.

In HAFELE's experiment the integrated components of time increase for one complete circuit of the earth were

	Time gain in nanoseconds	
	Eastward	Westward
Gravitational 'red shift'	144 ± 14	179 ± 18
Kinematic time dilatation	- 184 ± 18	96 ± 10
Predicted total time increase	- 40 ± 23	275 ± 21
Observed total time increase	- 59 ± 10	273 ± 7

Even for small velocities v at sea level the expression for Δt becomes $\Delta t = -\frac{R\Omega v t_o}{c^2} = -\frac{2\pi R^2 \Omega}{c^2} = -\frac{dV}{c^2}$ where d is the distance travelled ($2\pi R$) and V is the velocity of the rotating earth's surface. This result, which is independent of v, is identical with the time difference term in special relativity when time is coordinated by Einstein's convention using light signals. The discrepancy is of the opposite sign if the information is conveyed in the opposite direction. This is no problem but must always be calculated and allowed for.

To a good accuracy, clocks at rest at sea level keep the same relativistic time independently of latitude differences thus clocks conveyed around the Earth along a meridian at low velocity do not require correction (COCKE 1966).

The magnitude of the gravitational shift $\frac{gh}{c^2}$ is 1.09×10^{-13} per km. For two ground stations with substantial difference in altitude this effect cannot be ignored. The US Naval Observatory at Washington is responsible to the US Government for maintenance of the nation's time scales. However the National Bureau of Standards at Boulder is responsible for all standards of measurement including frequency and time interval. The US Naval Observatory controls Loran C emissions with the help of 16 selected commercial caesium clocks (WINKLER ET AL 1970) and thus has a major influence on the coordination of time throughout the northern hemisphere.

The NBS derives standard frequencies from a 3.66 meter caesium beam and broadcasts round the world (GLAZE 1970). In 1968 the two standards differed by 9.8×10^{-13} and a coordinated standard was agreed upon by subtracting a 1.8×10^{-13} correction due to the gravitational effect of the differing altitudes and then splitting the difference. In the forseeable future the 1.8×10^{-13} effect will be the predominant adjustment.

9. New Proposals For Frequency Standards

The standards that have been discussed have been in use for frequency and time measurement for a number of years and any immediate requirements would have to be satisfied by one or more of them. They are capable of further refinement but the limits are well understood. However it is to be expected that there will be major developments in the future as regards accuracy, size etc. arising from proposals that have already been made. Any attempt to plan long term centres for secular variation studies would require a study to be made of these future trends. It will not be possible here to do more than briefly outline a few of the more promising schemes and the progress to date (HELLWIG 1970 B; BASHKIN 1972).

10. Ion Storage Standard

The hydrogen maser selects and confines neutral atoms in a container and the limits of accuracy are due to collisions with the container walls and the tuning of the resonant cavity. A proposal has been made to confine massive hydrogen-like ions such as Hg^+ in a suitable configuration of electric fields and to make a passive frequency standard based on induced hyperfine transitions (SCHUESSLER 1971). A highly sophisticated technique is proposed in which the ions are produced in the trap by electron bombardment and then polarized by spin-exchange collisions with a beam of caesium atoms which itself has been fully polarized by the same means as used in a conventional caesium beam device.

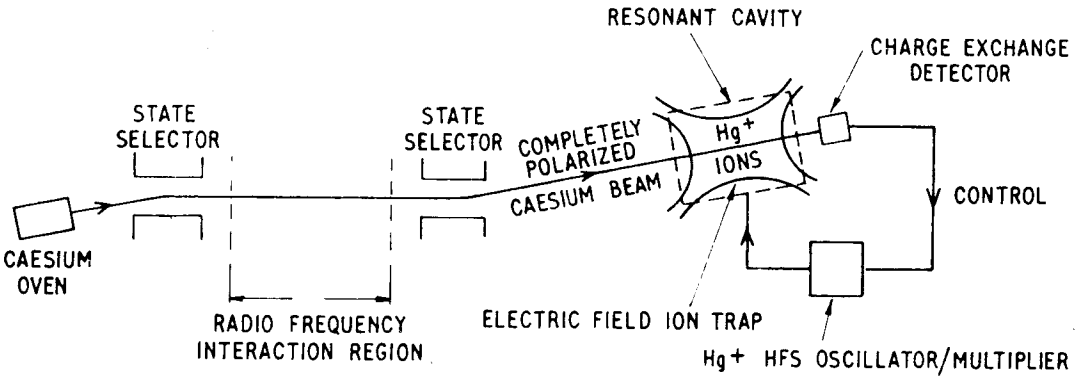

Figure 4. Hg^+ Ion Storage Frequency Standard

The effect of an applied radio-frequency field in inducing hyperfine transitions in the ions is then sensed by the effects (charge-exchange) of the same collisions with the polarized caesium beam. Some aspects of the proposal have been demonstrated using $(He^3)^+$ ions (SCHUESSLER ET AL 1969) and it is clear that there are many desirable features. Compared with the hydrogen maser the wall effect is calculated at parts in 10^{17} instead of 10^{11}. The hyperfine frequency is some 30 times higher and storage times are much greater. These both contribute to a very much higher line Q and the passive system reduces dependence on cavity tuning. All factors known to affect accuracy can be reduced to less than 1 in 10^{14} except the relativistic second order doppler shift $-\frac{v^2}{2c^2}$. This requires that the ion temperature be controlled to a few degrees. The proposal has many desirable features but will need a lot of proving and engineering if it is to leave a laboratory environment.

11. Atomic Beam Fine-Structure Standard

With the exception of the ammonia maser, existing atomic frequency standards rely on magnetic hyperfine structure. One reason for this is that microwave techniques have in the past restricted the radio frequencies to some tens of gigahertz, which is a very small energy difference when compared with normal electronic transitions. A new breed of standards is now being made possible by the progressive extension of radio techniques to much higher frequencies.

An atomic beam standard operating in the terahertz (10^{12}) region has been proposed and the forecast made of accuracy 'better than 10^{-15}'(STRUMLA 1972). The scheme (figure 5) utilizes a beam of neutral zero-spin atoms such as Mg or Ca which are excited by a discharge inside the oven to the lowest excited state, a metastable triplet P level.

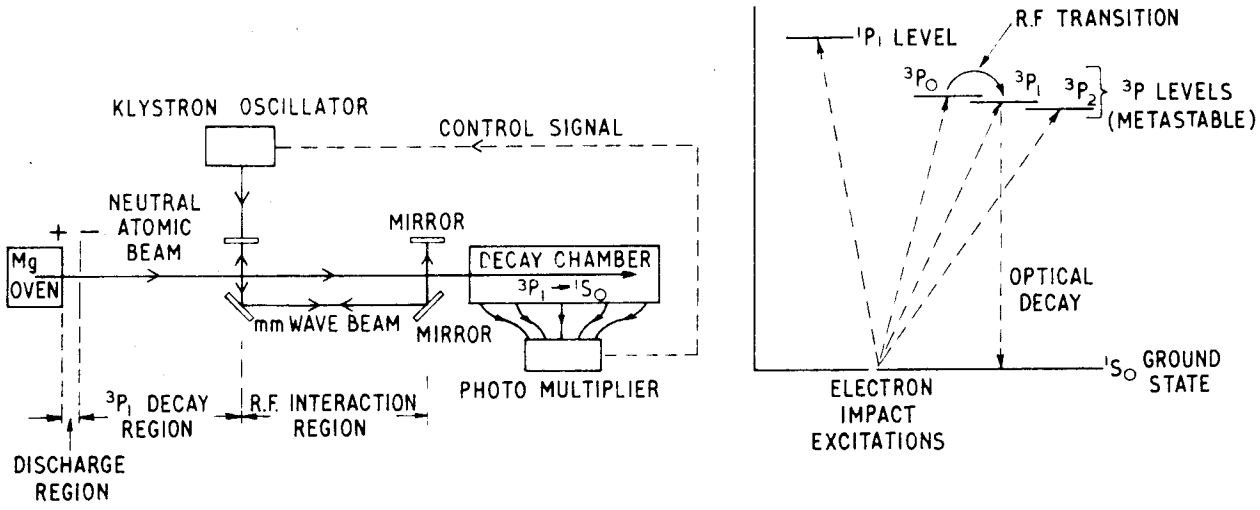

Figure 5. Mg Beam Fine Structure Frequency Standard

The $^3P_1$ state is not very long lived and decays to the ground state in milliseconds leaving $^3P_0$ and $^3P_2$ atoms in the beam which then passes through an interaction region where magnetic fine-structure transitions are induced between the $^3P_0$ and $^3P_1$ levels by an appropriate radio frequency field (601 GHz for Mg, 1564 GHz for Ca). The $^3P_1$ atoms so formed decay rapidly to the ground state emitting photons which serve as an indicator of the resonance of the applied frequency. The line width as with all beam standards is determined by the interaction time and the frequency is 100 times higher than for caesium so the line Q and the stability are increased 100 fold. Once again an important limitation of accuracy is set by the second order doppler shift.

12. Stabilized Laser Standards

There is intense activity at present to stabilize optical and infrared lasers to accuracies comparable with the frequency standards that have been discussed. In parallel with this, the interlocking of microwave and laser frequencies is gradually being achieved by an extension of traditional radio techniques (BRADLEY ET AL 1972; BOYNE 1971). The methods are cumbersome and impermanent as yet and typically involve the stabilization and interlocking of several intermediate maser and laser oscillators using Schottky diode multiplier/mixers. It is not impossible however that a simple, well engineered standard with associated electronics will be achieved within the next few years and may serve to define both length and time standards in the same instrument.

Traditionally the Fabry-Perot type lasers have been stabilized by accurate control of the mirror spacing using the 'Lamb dip' of the gain/frequency profile as an indication of resonance. This dip arises because, in general, moving molecules experience a doppler shifted electromagnetic field and only those molecules with a particular velocity are necessarily resonant with the field. If the field is exactly right the resonance occurs only with molecules having little or no component of velocity in the direction of the laser beam. Such molecules will resonate with the laser beams in both directions at the same time and hence experience greater saturation effects. This can show up as a dip at the centre of the doppler broadened resonance line. It is possible to produce a similar effect by inserting an absorbing medium outside the discharge region but inside the optical resonator (figure 6). In this case saturation of the absorption occurs giving rise to an emission effect when the laser is tuned close to the centre of the absorption resonance. If the absorbing level of the molecules has a long natural lifetime and the optimum pressure is used, the saturated absorption linewidth can be a magnitude or so narrower than the normal Lamb dip giving rise to a more accurate indicator for control of frequency. This has been done most successfully with the He-Ne laser and a CH_4 absorber (BARGER & HALL 1969) leading to a reproducibility of 10^{-11} and a stability of 10^{-13} over a 10 s averaging time (BAY ET AL 1972; HELLWIG ET AL 1972). The latest stability results are shown in figure 8 superimposed on those of other standards.

There are other possibilities with different lasers and absorbing media and very promising results have already been achieved leading to more accurate determinations of the velocity of light (EVENSON ET AL 1973; BARGER & HALL 1973). Even greater frequency stability is proposed by the use of the absorption cell technique in a ring laser (BASOV ET AL 1971).

Other proposals have been made for optical laser stabilization by interrogating conventional atomic beams (BASHKIN 1972). In one of these (ORAEVSKY 1968), the rf interaction region of a caesium beam device is replaced by a similar Ramsay-type interaction region with an optical system arranged so that the atomic beam crosses the laser beam twice at right angles (figure 7).

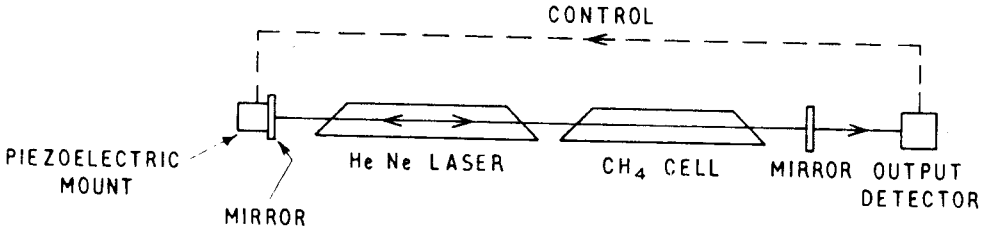

Figure 6. Methane Stabilized He Ne Laser

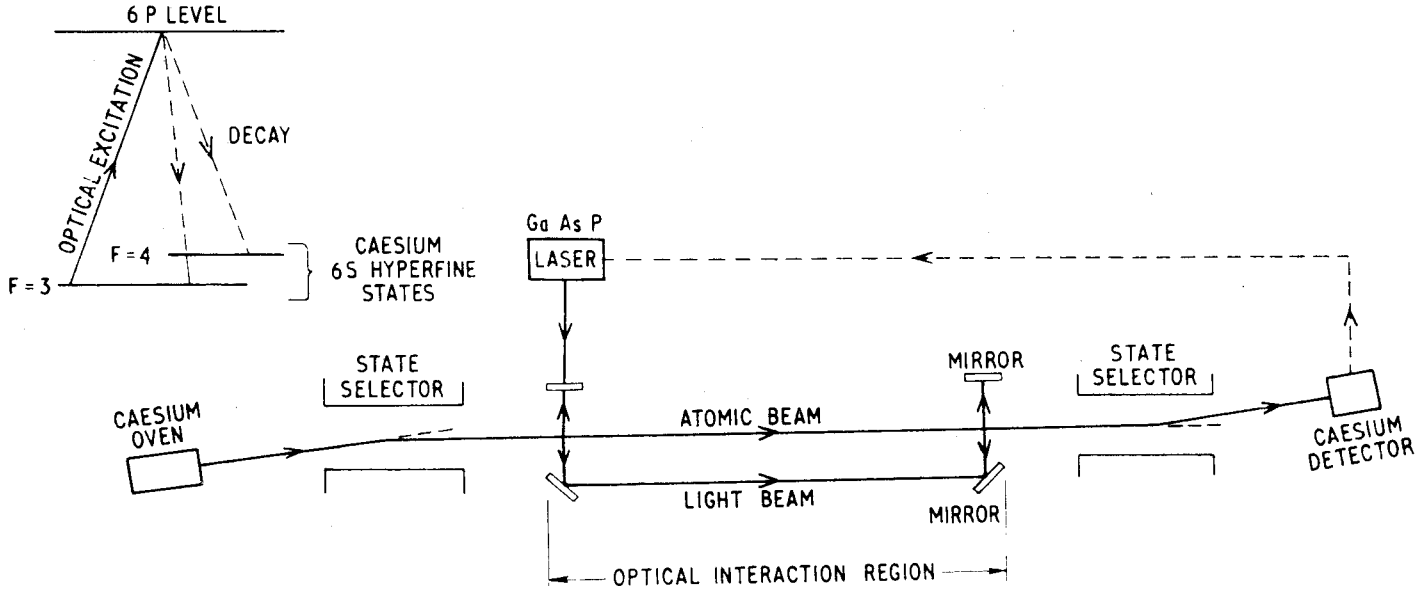

Figure 7. Laser Stabilization By Atomic Beam

In this case a GaAsP solid state laser would provide a suitable frequency to excite the caesium atoms of the selected hyperfine state to a 6P level. The atoms would decay rapidly back to the 6S ground state but would populate the empty hyperfine level and give rise to a signal in the output beam detector.

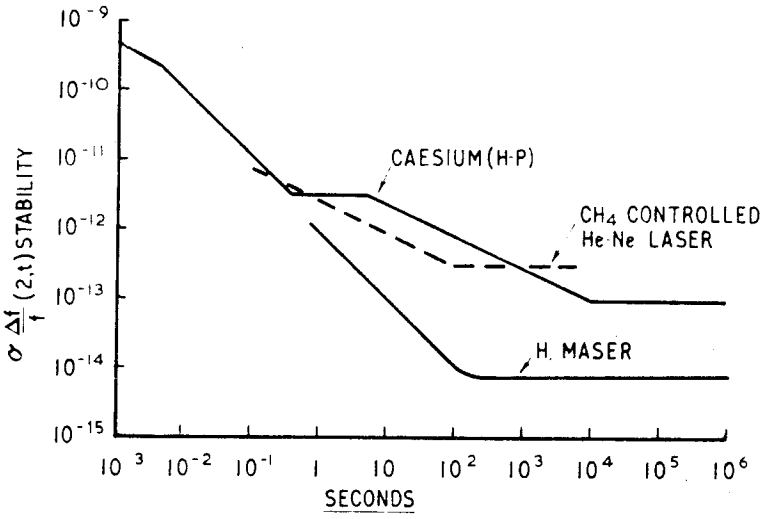

Figure 8. Methane - Stabilized Laser

13. Conclusion

There is an embarrassingly large number of proposals for the next generation of frequency standards with accuracy potentials exceeding 10^{-13}. It is likely that one at least of these will achieve the claims made for it and at the same time equal or improve on the best existing accuracy and stability and provide a compact, transportable device comparatively insensitive to magnetic fields and other environmental effects. For the next few years, however, reliance must be placed on the proven existing devices with rubidium standards for bread and butter requirements too demanding for quartz crystals, commercial caesium beams for more important purposes, and hydrogen masers for long baseline interferometry.

A long term research facility for secular variation studies would probably require all three of these devices.

14. References

BARGER, R. & HALL, J. 1969. *Phys.Rev.Letts*, 22, No. 1: 4.

BARGER, R. & HALL, J. 1973. *Appl.Phys.Letts*, 22, No. 4: 196.

BASHKIN, A. 1972. *Soviet J.Quantum Electronics*, 1, No. 5: 437.

BASOV, N., BELENOV, E., DANILEIKO, M. & NIKITIN, V. 1971. *Soviet J.Quantum Electronics*, 1, No. 1: 28.

BAY, Z., LUTHER, G. & WHITE, J. 1972. *Phys.Rev.Letts*, 29, No. 3: 189.

BEEHLER, R., MOCKLER, R. & RICHARDSON, J. 1965. *Metrologia*, 1, No. 3: 114.

BOYNE, H. 1971. *IEEE Trans.Instrum. Measmt*, IM-20: 19.

BRADLEY, C., EDWARDS, J., KNIGHT, D., ROWLEY, W. & WOODS, P. 1972. P. 295 *Atomic Masses & Fundamental Constants 4* (ed. J. Sanders and A. Wapstra) Plenum Press, London.

BRENNAN, J. 1971. *Proc.Precise Time & Time Interval, Strategic Planning Mtg*, 1: 305 (US Naval Observatory).

COCKE, W. 1966. *Phys.Rev.Letts*, 16: 662.

EVENSON, K., WELLS, J., PETERSEN, F., DANIELSON, B. & DAY, G. 1973. *Appl.Phys.Letts*, 22, No. 4: 192.

GLAZE, D. 1970. *IEEE Trans.Instrum.Measmt* IM-19, No. 3: 156.

HAFELE, J. 1972. *Science*, 177, No. 4044: 166, 168.

HELLWIG, H. 1970 A. *Metrologia*, 6, No. 2: 56.

HELLWIG, H. 1970 B. *Metrologia*, 6, No. 4: 118.

HELLWIG, H., VESSOT, R., LEVINE, M., ZITZEWITZ, P., ALLAN, D. & GLAZE, D. 1970. *IEEE Trans. Instrum.Measmt* IM-19, No. 4.

HELLWIG, H. & BELL, H. 1972. *Metrologia*, 8:96.

HELLWIG, H., BELL, H., KARTASCHOFF, P. & BIRGQUIST, J. 1972. *J.Appl.Phys.* 43, No. 2: 450.

KLEMPERER, W. 1972. *Proc.IEEE*, 60, No. 5: 602.

LEVINE, M. & VESSOT, R. 1970. *Radio Science*, 5, No. 10: 1287.

LURE Team 1970. *Science*, 167: 458.

MATHUR, N., GROSSI, M. & PEARLMAN, M. 1970. *Radio Science*, 5, No. 10: 1253.

MOCKLER, R. 1961. *Advances in Electronics and Electron.Phys.* 15.

ORAEVSKY, A. 1968. *IEEE Trans.Instrum Measmt*, IM-17, No. 4: 346.

RAMASASTRY, J., ROSENBAUM, B., MICHELINI, R & KUEGLER, G. 1973. *IEEE Trans.Instrum.Measmt*, IM-22, No. 1.

RAMSEY, N. 1965. *Metrologia*, 1, No. 1: 7.

RAMSEY, N. 1972. *IEEE Trans.Instrum.Measmt* IM-21, No. 2: 90.

SCHUESSLER, H., FORTSON, E. & DEHMELT, H. 1969. *Phys.Rev.* 187: 5.

SCHUESSLER, H. 1971. *Metrologia*, 7, No. 3: 103.

SMITH, H. 1972. *Proc.IEEE*, 60, No. 5: 479.

STRUMLA, F. 1972. *Metrologia*, 8: 85.

VESSOT, R., LEVINE, M., ZITZEWITZ, P., DEBELY, P. & RAMSEY, N. 1970. P. 27, *Proc.Int.Conf. Precision Measurement and Fundamental Constants, August 1970*, at National Bureau of Standards, Gaithersburg, Md, USA. (ed. Langenberg and Taylor).

WINKLER, G., HALL, R. & PERCIVAL, D. 1970. *Metrologia*, 6: 126.

WINKLER, G. 1970. *Proc.Precise Time & Time Interval (PTTI), Strategic Planning Mtg*, 1: 129 (US Naval Observatory).

ZITZEWITZ, P. & RAMSEY, N. 1971. *Phys.Rev.* A3: 51.

15. Discussion

WHITTEN (Chairman): I wish to mention some work that was done in the Cascade Mountains (USA). There is a tunnel there available to physicists at the University of Washington. VALI & BOSTROM used a hydrogen maser to control the strain experiment for which they used a laser interferometer. They found there was a sudden step change. This emphasizes the necessity for redundancy such as you have pointed out. They assumed that in this case, it was the hydrogen maser and not some sudden step change in the strain field.

HIBBARD: The hydrogen maser could have had automatic tuning. Automatic tuning causes changes in the frequency.

GUBBAY: You mentioned the sensitivity to Doppler in some of these lasers. Which of them is least sensitive and why aren't they all as sensitive?

HIBBARD: Do you mean lasers or atomic beam devices?

GUBBAY: Atomic beam devices.

HIBBARD: Firstly, you have to know the velocity as they come out of the hole. If you don't know the velocity, a thermal distribution is assumed. That's not quite right. You collimate. A good long collimator is what you like; you then get a different system. The slower atoms are knocked on by the faster ones. You've got to know the velocity distribution. The hydrogen maser is the only device where you know that.

GUBBAY: Wouldn't you get interaction between particles which would destroy the monochromatic light?

HIBBARD: It is not monochromatic. An atom is being "scanned" for half a second or so and is changing its velocity after each collision. First order Doppler effects cancel out. In the case of the caesium beams, you get a Doppler reduction by "scanning" at right angles. The original ammonia maser effectively "scanned" in length.

WHITTEN: Thank you for preparing your paper which I am sure will serve as a reference document for some time.

NASON, R.D.*
U.S. Geological Survey
Menlo Park, California
United States of America

Proc. Symposium on Earth's Gravitational Field & Secular Variations in Position (1973),637-639.

OBSERVATION SITES FOR SECULAR VARIATION STUDIES *

ABSTRACT

In an astronomical Earth-surveying program using movable telescopes to study Earth deformation, the usefulness of the measurements will depend on the long-term stability of the permanent survey marks. In areas of weak rock or soil on sloped ground, there will be a tendency for the survey mark to move slowly downhill. In areas where underground oil or water is being withdrawn, the ground surface may "subside", together with horizontal movements. Seasonal moisture or freezing changes in soil can cause movements of several centimetres.

Most causes of local instability can be avoided by careful installation of survey marks. But for complete certainty, the local position of an astronomical survey mark should be carefully measured to nearby or distant reference marks using geodetic triangulation, trilateration, and/or levelling. If local movement does occur, the reference measurements will show the amount of movement for a site correction. Having the astronomical survey mark be part of an existing geodetic network, or extending an existing network to the observation site, will improve the value of the results.

1. Text *

I am very sorry that Dr. Nason cannot be here to speak on "Observation Sites for Secular Variation Studies". Bob Nason is a good friend and colleague of mine. He has shown a very keen interest in searching for and locating those special areas where fault creep may be observed and measured. I will not attempt to give you his thoughts on the subject assigned to him but for a few moments I wish to describe some aspects of the crustal movement program in California and the relevance of some of the discussion we have had this week.

More than 40 years ago, seismologists in California who were working with geodesists in developing a program for detecting crustal movement, recommended establishing eight traverse or triangulation schemes crossing the San Andreas Fault system. Near the fault, monuments were spaced 25 m apart, then at 50 and 100 m spacing and eventually at 1 to 2 km for a total distance of 25 or more km on each side of the fault. The closer spacings were designed for the use of 50 m invar tapes but, unfortunately, many of the sites were not ideally located. Many marks were damaged or destroyed by highway development, etc. The original program specified a re-survey every ten years or an immediate re-survey following an earthquake. Through the years additional networks were established, some for monitoring crustal movement but many for the overall requirement of geodetic control for large scale mapping, highway construction, etc. Today, there are about 10,000 geodetic points throughout this area. Many of them are monitored on a repeat basis to detect crustal deformation. Crustal deformation occurs in relatively short wavelengths in comparison to the total extent of the area.

---

* Text is that of a talk given by C.A. WHITTEN, Chairman of Session L, in lieu of the paper by R.D. NASON who was unable to attend.

I will quickly review what has been learned concerning movement along the broad San Andreas system. North of San Fransisco, near Fort Ross, repeat surveys show strain accumulation at a rate approximating 1 in 10^6 per year. There is no evidence of creep. Near San Fransisco, the San Andreas fault seems to be locked, but on the east side of the Bay there is evidence of creep of a few mm per year along the Hayward and Calaveras faults. Further south, near Hollister, the rate increases to 12 to 14 mm per year and near Cholame the rate of creep is as large as 35 mm per year. Near the bend in the fault system at the junction with the Garlock fault, there is evidence of north-south compression and in the piece of pie shaped segment between the two faults there is evidence of elongation. Repeat geodetic levelling indicates subsidence in this latter block. The horizontal measurements show a slight left lateral creep on the Garlock fault but the major system seems to be locked. Near the southern end of the system, there is evidence of continuing movement across the Imperial Valley. Some of this movement may be creep along the various faults that comprise the total system in this region. There is an urgent need for more closely spaced survey points and more frequent monitoring.

Two weeks ago there was a crustal movement symposium in Bandung, Indonesia. James Savage presented a paper on work being done by the U.S. Geological Survey on the west side of the San Andreas fault near Hollister. They have a network of nine points concentrated in a region about 5 km on a side. The measurements indicate that if there is any strain accumulation it is only about 2 in 10^7 per year. They are using a Geodolite for the measurements. Recently I saw a demonstration of a new distance measuring instrument called the Mekometer. It is available to geodesists and can measure distances to 1 part in 10^7. Seismologists are asking geodesists to measure distances accurate to a millimetre or a fraction of one. When we think in terms of how 1000 km laser range baseline measurements accurate to 3 or 4 cm might be used, such lines would be of tremendous assistance to the geodetic community for controlling the accumulation of error that occurs in the classical geodetic networks.

I want to refer to another paper presented at Bandung. Dr. Fujita, who is present here, presented a very interesting paper on the re-triangulation in Japan. After listening to the discussion on collocation techniques this week, I am suggesting a variation in technique which might be applied by geodesists in the United States or in Japan. Dr. Fujita used the primary triangulation net in Japan, adjusting two sets of observations, separated by approximately 60 years. He held six points "fixed" along the full length of the country. Of course, this produced some distortion. I wish to suggest a technique which would essentially hold all points fixed. Then look at the corrections to the observed directions, treating them in a statistical manner such as Moritz and his colleagues have suggested. Use the differences of corrections to directions to determine strain accumulation. Where there are discontinuities, earthquakes have occurred. Those values would determine strain release.

It may be that some slight variation in this procedure is necessary. But following the philosophy of holding all points fixed, because of the strength obtained in combining observational data, permit some slight relaxation at those points where the corrections from this adjustment process indicate that relaxation should occur. It would require an inverse sigma type of application plus iterative computations to arrive at optimum results. I am convinced this type of study is worthwhile. Strain accumulation follows a systematic pattern. Where there are discontinuities, these are clearly defined as the displacements which occur at the time of an earthquake. The signal to noise ratio is such that the noise is often a little greater than the signal we are seeking. Thus, considerable expertise in statistical methods is required to obtain meaningful results.

I suggest this as something I gained from this symposium this week and hope it might be applied to blocks of geodetic data in attempting to get a clearer picture of what happens in crustal deformation.

KAULA, W.M.
Department of Planetary & Space Science
University of California
Los Angeles, California 90024
United States of America

Proc.Symposium on Earth's Gravitational Field & Secular Variations in Position (1973),640-642.

MOTIONS INFERRED FROM REMANENT MAGNETISM, FRACTURE ZONE ORIENTATIONS, AND EARTHQUAKE SLIP VECTORS

1. Text

For tectonic plates of more than 5000 km extent, the standard deviations of relative motion determinations are less than 0.6 cm/year. This uncertainty applies to the motion averaged over the last five million years. Within the accuracy of the data, the motion has been steady for the last ten million years. The resolution of the remanent magnetic data is about 100,000 years.

In a symposium discussing secular variations in position, it seems appropriate to review the evidence which has persuaded most solid Earth geophysicists that major segments of the Earth's lithosphere are moving at steady rates on the order of 5 cm/yr with respect to each other. A knowledge of the accuracy and limitations of these determinations is necessary to plan the application of geodetic techniques most effectively to these problems. Fortunately such a review is facilitated by the recent comprehensive analysis of MINSTER ET AL (1974). Their analysis synthesizes and updates the determinations of the four classic papers, (MCKENZIE & PARKER 1967), (MORGAN 1968), (LE PICHON 1968) and (ISACKS ET AL 1968), which clinched the plate tectonics revolution.

The study by MINSTER ET AL (1974) analyzed three data types:

- remanent magnetic stripes centred on ocean rises;
- oceanic fracture zones; and
- seismic slip vectors.

The analysis was extremely detailed and thorough: the paper is 57 pages long and has 121 references. Special attention was paid to statistical techniques, and iterative procedures were used to avoid convergence to non-global optima.

The first data type was measurement of magnetic fields on 68 profiles across ocean ridges. For these data, the digitization interval is 1.7 km, corresponding on the average to about 30,000 years of sea floor spreading. Since it takes more than one data point to infer a variation and since there is some variation in signal strength due to topographic irregularities, lithological variations, etc, the true resolution is conservatively estimated to be about 100,000 years. For regions of average or rapid spreading, data out to magnetic anomaly three (about five million years) were used, and for regions of slow spreading, data to anomaly five (ten million years) were used. For comparisons with radiometrically dated magnetic intensity sequences, the marine magnetic profiles are corrected for both latitude and orientation.

The second data type was orientation of 62 oceanic fracture zones: locations where oceanic rises are offset by strike-slip fractures. If these fractures are strike-slip, and if the plate motions are rigid, then the fractures must lie along parallels about the pole of rotation between plates. Hence

each fracture zone orientation is an estimate of the rotation pole, but not of rate.

The third data type was 106 earthquake slip vectors. When an earthquake occurs, it is expressible as a double couple. There is a break in the material and motion of the material on one side of the break with respect to the other, but there is no nett volumetric change from an earthquake. In the signal radiated from an earthquake, in two quadrants the onset of the longitudinal P wave will coincide with a dilatation, and in the other two, to a compression. The systematic variations with azimuth in an earthquake of this initial signal are analysed to get the direction of motion of the earthquake.

In three dimensions there is an ambiguity -- there are two principal directions in which an earthquake could occur. At this point, geological interpretation is used to determine which nodal direction is reasonable. In the case of strike-slip faults like the San Andreas, it is obvious that the motion does not occur at right angles to the fault. In faults which involve under thrusting, the determination is less strong. In the analysis by Minster and co-workers, it was arbitrarily assumed that no slip vector is known to better than 10°.

The analysis took into account twelve plates:

- the LE PICHON (1968) six (Pacific, Americas, Eurasia, India, Antractic, and Africa),
- plus separation of South America from North America,
- the Nazca and Cocos plates separate from an Antarctic, and
- the Arabian plate from the Eurasian.

The slip vectors also indicate a Bering plate separate from the North American. The twelfth plate was the Somali plate whose motion with respect to the African plate could not be discriminated from zero. Minster et al were very careful to omit any slip vectors which caused any confusion at all. For example they omitted all seismic data along the Alpide belt from the Mediterranean to New Guinea.

Any motion of points on a sphere relative to each other can be described as rotation about a specific pole, so locations of these poles as well as rates of rotation are required. Since the location of the pole is defined by sines and cosines of latitude and longitude, the problem is non-linear. It is possible to converge from a least squares solution to a false minimum. The procedure adopted by MINSTER ET AL (1974) was first a solution for relative motion between triplets of plates. Next, from best solutions for these sets of triplets, for quadruplets of plates. Finally they worked stepwise to a set of 12 plates. In this process, they made findings about separating off the Bering and South American plates from the North American plate and so forth. For plates of more than 5000 km (all except Cocos, Arabia and Bering), the standard deviation of relative motion averages ±0.3 cm yr^{-1}. The maximum for major plates is ±0.6 cm yr^{-1}. The uncertainties for the Cocos and Arabic plates are ±1.2 cm yr^{-1}. The distribution of the residuals fits a chi-square test very well.

In two places, comparisons with geodetic data can be made. In Tadzhikistan, the closure rate between the Indian and Eurasian plates is 3.8 cm yr^{-1}, compared to the 2.0 cm yr^{-1} measured on the Hissaro fault. In California, the slip rate between the North American and Pacific plates is 5.5 cm yr^{-1}, compared to 3.2 cm yr^{-1} measured on the San Andreas fault. In both these places, about half the motion is obviously being taken up by complexes of subsidiary faults about the main fault.

A second analysis by MINSTER ET AL (1974) estimated motion relative to an absolute frame. They adopted the hot spot hypothesis and at 20 places in the world, such as the Hawaiian volcano chain,

used radioactive dating as a guide to the rate and direction of motion of the plate with respect to a set of hypothetical hot spots. They used seven chains in the Pacific, three in the Indian Ocean, five in the south Atlantic, three in the north Atlantic and two in North America.

These chains were carried back ten million years, twice as long as used for relative analysis. From a best fit, an estimate of absolute motion was obtained. The internal uncertainty of the results was less than 1 cm yr^{-1}. There are three interesting things about this hot spot frame.

1. It coincides very closely with the frame defined by minimizing the velocity normal to compressive belts of the over-riding plates, i.e., the typical situation being an oceanic plate going underneath a continental plate. In this case, the continental plate is staying still and the oceanic plate is the one that is moving.
2. It is very close to minimizing the nett rotation of the entire lithosphere.
3. It is close to a frame minimizing continental motion and maximizing oceanic motion.

The task of geodetic techniques is thus to measure variations from the steady states determined mainly from remanent magnetism. Considering that

1. the motions from earthquake slip vectors over the last seventy years agree fairly well with those from remanent magnetism (DAVIES & BRUNE 1971); and
2. earthquakes are not known to extend more than 1000 km (KELLEHER ET AL 1973),

it is probable that measurable variations in motion are confined to zones of less than 1000 km width about plate margins.

2. References

DAVIES, G.F. & BRUNE, J.N. 1971. Regional and Global Fault Slip Rates from Seismicity. *Nature Physical Science* 229,101-107.

KELLEHER, J., SYKES, L. & OLIVER, J. 1973. Possible Criteria for Predicting Earthquake Locations and Their Application to Major Plate Boundaries of the Pacific and the Carribean. *J.geophys.Res.* 78,2547-2585.

MCKENZIE, D.P. & PARKER, R.L. 1967. The North Pacific: An example of Tectonics on a Sphere. *Nature* 216,1276-1280.

ISACKS, B., OLIVER, J. & SYKES, L.R. 1968. Seismology and the New Global Tectonics. *J.geophys.Res.* 73,5855-5899.

LE PICHON, X. 1968. Sea Floor Spreading and Continental Drift. *J.geophys.Res.* 73,3661-3697.

MINSTER, J.B., JORDAN, T.H., MOLNAR, P. & HAINES, E. 1974. Numerical Modeling of Instantaneous Plate Tectonics. *Geophys.J.R.astr.Soc.* (in press).

MORGAN, W.J. 1968. Rises, Trenches, Great Faults, and Crustal Blocks. *J.geophys.Res.* 73,1959-1982.

3. Discussion

DOOLEY: One phenomenon which is prominent in sea floor spreading is that the spreading on each side of an oceanic ridge is quite symmetrical. Has this been used?

KAULA: Symmetry has not been assumed. The results obtained are consistent with symmetry, however.

GRAFAREND, E.W.
Institut für Theoretische Geodäsie
University of Bonn
Bonn
Federal Republic of Germany

Proc.Symposium on Earth's Gravitational Field & Secular Variations in Position (1973) ,643-659.

A LOD AND WOBBLE ANALYSIS OF GENERALIZED EULER-LIOUVILLE TYPE BASED ON VIRIAL PLANETARY EQUATIONS

ABSTRACT

Four dimensional geodesy is based on longitude, latitude and gravity variations in time. The classical analysis of the length of day (LOD) and of the Earth's wobble has its origins in the Euler - Liouville equation. For three different Earth models (rigid, liquid, elastic) the virial method as an alternative tool is applied to generalize the Euler - Liouville problem. Numerical solutions are are discussed for the different models.

1. Introduction

Geodesy can be understood as the science defining estimable, unique space-time co-ordinates, especially of points on the surface of the Earth or other planets. There are two central problems characterizing geodesy:

- the problem of finding *holonomic* space-time co-ordinates; and
- the geodetic *datum* problem.

In three dimensional geodesy these problems are the following:
All geodetic instruments, for example levelling instruments, theodolites, gyro-compasses. satellite cameras, satellites, refer to gravitation. Related to the *local* gravity vector the so-called "natural" or astronomical co-ordinate system is introduced; therefore the local measurement triad (east, north, vertical), which is orthonormal, characterizes this system. But it is easy to prove that co-ordinates measured along these axes are *anholonomic*, non-integrable, therefore non-unique. The determination of co-ordinate differences between two points is path-dependent. In order to give an example we note that the Cartesian co-ordinate differences along east,north, vertical, calculated from measurements of the azimuth, the vertical angle, and the distance, are non-integrable. There is no way to arrive at *global* unique co-ordinates from co-ordinate differences if we have no further information about the size and shape of the gravity field. In geodesy, two ways have been gone to change this situation. A.Marussi introduced in 1949 the three co-ordinates astronomical longitude, astronomical latitude and geopotential and proved that these co-ordinates are *holonomic*. He succeeded in transforming co-ordinate differentials from the natural triad into the mentioned holonomic one by introducing in general, nine integrating factors of the Pfaff-Frobenius-Cartan type. This transformation, today called the Marussi transformation, is characterized by gravity gradients and the Euclidian norm of the gravity vector. For more details see (GRAFAREND 1971;GRAFAREND 1972; GRAFAREND 1973a,b,c). In geodesy, the Marussi co-ordinate system was not a breakthrough for practice. The *geocentric* co-ordinate system along the triad to Greenwich, orthogonal to Greenwich, and parallel to the rotation vector of the Earth *turned out to be holonomic*, alternatively. This frame had the advantage to coincide with our natural feelings about the embedding of the Earth in a three dimensional Euclidian world.

The Pfaff-Frobenius-Cartan type of transformation from co-ordinates along the natural anholonomic triad into the holonomic geocentric triad depends only on the local astronomical longitude and astronomical latitude. Added to the three natural co-ordinates along east, north, vertical, we have a five dimensional geodetic concept! The *geodetic datum problem* has its origin in the fact that we can measure only co-ordinate differences, but we have to know global co-ordinates. A geodetic net must be fixed for translation, rotation and scale. Free net adjustment problems with singular normal equations are typical.

Classical three-dimensional geodesy is based on the assumption of a rigid Earth. This is a very good first order approximation, but modern geodetic concepts reflect this restriction. Of course, we have crustal movements etc for a real non-rigid Earth. Time dependent or four-dimensional co-ordinates have to be introduced. The question of holonomity and datum are very open for discussion.

Against this background, we introduce the most general four-dimensional continuum concept at this point. For a plastic-elastic Earth, we will refer to four-dimensional moving frames (4D-Cartan frames) of, in general, anholonomic type in section 2. The concept of dislocation is included.

All text books referring to the dynamics of such a continuum, introduce the so-called Euler-Liouville equation plus some intuitive feeling how the inertial moments change with the rotational speed of the Earth, and some parameters characteristic of the mechanical behaviour - the Love numbers. This concept has the disadvantage not to reflect to the now classical theory of plasticity and elasticity. For example, in elasticity Lame's constants or another set of two constants describe an isotropic material. The main difficulty in deriving a second order dynamical equation, the moment of momentum, is the fact that the vector form of this moment is independent of plastic-elastic effects. In section 3 we present our solution to this problem: the technique of tensorial virial equations. We succeed in formulating a general dynamic equation for a plastic-elastic-liqiud-viscous body, including couple stress. This is an important tool to introduce the hydromagnetic coupling of the core and the mantle of the Earth.

Sections four to six are examples of different mechanical models. We start with rigid body displacements and calculate the free precession of the Earth. Then we study Maclaurin type equilibrium figures for liquid body displacements. Finally we describe the second order dynamic virial equation of second rank tensor type for an elastic body displacement which includes Lame's constants!

2. Four Dimensional Moving Frames (4D-Cartan Frames)

The material points of a continuous medium at the ideal or initial state (at time zero) occupy a region B that consists of the material volume V and the surface S. The position of a material point P in this region is denoted by a curvilinear co-ordinate X^K, K=1,2,3, or by a vector P that extends from an origin O of the co-ordinates to the point P. After the total deformation (plastic and elastic deformation) takes place, at time t, the material point of V + S go into a region b consisting of a spatial volume v and its surface s. A point p in the deformed or final state may be represented by a new set of curvilinear co-ordinates x^k, k=1,2,3, or a position vector p that extends from the origin C of the new co-ordinates to the point p. Often it is advantageous to select these two reference frames to be non-identical. In the description of *motion* of a continuous body, we shall find a definite need for the use of these two types of co-ordinates. Following the current terminology, we shall call X^K the material or *Lagrangian* co-ordinates and x^k the spatial or *Eulerian*

co-ordinates. The position vector $\mathbf{P}$ of a point P in B and $\mathbf{p}$ of one in b referred respectively to rectangular co-ordinates Z^K and z^k, are given by

$$\mathbf{P} = Z^K E_K \quad , \qquad \mathbf{p} = z^k e_k \qquad 2(1),$$

where E_K and e_k are the rectangular base vectors in Z^K and z^k. Of course, there is a mapping $Z^K(X)$ and $z^k(x)$. For example, the base vectors e_k at time zero can be directed to the mean ecliptic (1950.0) system. Infinitesimal vectors $d\mathbf{P}$ in B and $d\mathbf{p}$ in b may be expressed as

$$d\mathbf{P} = G_K dX^K \quad , \qquad d\mathbf{p} = g_k dx^k \qquad 2(2),$$

where in general for *anholonomic co-ordinates* $G_K \neq \partial P/\partial X^K$ and $g_k \neq \partial p/\partial x^k$. The situation is very typical for geodetic problems. In 1972 I proved that co-ordinates along the "natural" triad east, north, vertical are anholonomic. If F is the Frobenius matrix of integrating factors mapping the anholonomic co-ordinates dX onto the holonomic co-ordinates dZ one-to-one; F: $dX \rightarrow dZ$, the transformation of the base vectors is due to

$$G_K = F_K^M E_M \quad , \qquad g_k = f_k^m e_m \qquad 2(3).$$

The base vectors $G_K(X)$ and $g_k(x)$ are moving frames of the 3D type. Their parameters are the three components of their position vector. The deformed or final infinitesimal vector $d\mathbf{p}$ consists of the *plastic* part $d\mathbf{p}_{plast}$ and the *elastic* part $d\mathbf{p}_{el}$.

$$d\mathbf{p} = d\mathbf{p}_{plast} + d\mathbf{p}_{el} \qquad 2(4)$$

defined by the line integrals

$$\oint d\mathbf{p} \neq 0 \quad , \qquad \oint d\mathbf{p}_{plast} \neq 0 \quad , \qquad \oint d\mathbf{p}_{el} = 0 \qquad 2(5).$$

In order to understand better these two fundamental types of deformation, let us refer for a moment to holonomic co-ordinates Y^K, and thus base vectors $H_K = \partial P/ Y^K$. Y^K may be represented by the holonomic Marussi co-ordinates astronomical longitude, astronomical latitude and geopotential at the initial state. The misclosure of the plastic infinitesimal vector $d\mathbf{p}_{plast}$ is due to Cartanian torsion. The squares of the lengths of the infinitesimal vectors $d\mathbf{P}$ and $d\mathbf{p}$ in B and b are respectively

$$dS^2 = d\mathbf{P}\cdot d\mathbf{P} = G_{KL}\, dX^K\, dX^L, \qquad ds^2 = d\mathbf{p}\cdot d\mathbf{p} = g_{k\ell}\, dx^k dx^\ell \qquad 2(6).$$

$$G_{KL}(X) = G_K \cdot G_L \quad , \qquad g_{k\ell}(x) = g_k \cdot g_\ell \qquad 2(7)$$

are the covariant metric tensors of B and b respectively. For comparison purposes it will often be necessary to *shift* vectors and tensors to the same system in parallel transport. For example, by definition, components of position vectors $\mathbf{P}$ and $\mathbf{p}$ in X^K and x^k

$$P^K = \mathbf{P}\cdot G^K \quad , \qquad p^k = \mathbf{p}\cdot g^k \qquad 2(8).$$

Suppose now we want to shift $\mathbf{p}$ to the point P(X) in parallel transport. If p^K are the components of $\mathbf{p}$ in X^K, then

$$p = p^K G_K(X) = p^k g_k(x) \qquad 2(9)$$

or by taking inner products with G^L and g^ℓ, we get

$$p^K = g^K_{.k} p^k, \qquad p^k = g^k_{.K} p^K \qquad 2(10),$$

where

$$g^K_{.k}(X,x) = G^K(X) \cdot g_k(x), \qquad g^k_{.K}(X,x) = g^k(x) \cdot G_K(X) \qquad 2(11)$$

are the *shifters* required for this parallel transport. The shifters relate components of a vector in two co-ordinate systems. They are *two-point* tensor fields. We say that *a body has undergone a rigid-body displacement wherever* $ds^2 = dS^2$ *for all material points.* Therefore the difference $(ds^2 - dS^2)$ is a measure of the deformation produced during a displacement. If at time t, we look upon the motion

$$dX^k = A^k_K \, dX^K, \qquad dX^K = A^K_k \, dx^k \qquad 2(12),$$

then by substitution we get

$$dS^2 = c_{k\ell}(x,t) \, dx^k dx^\ell, \qquad ds^2 = C_{KL}(X,t) \, dX^K dX^L \qquad 2\,(13)$$

for all

$$c_{k\ell} := G_{KL}(X) \, A^K_k \, A^L_\ell \qquad 2(14)$$

$$C_{KL} := g_{k\ell}(x) \, A^k_K \, A^\ell_L \qquad 2(15),$$

then

$$ds^2 - dS^2 = 2E_{KL}(X,t) \, dX^K dX^L = 2e_{k\ell}(x,t) \, dx^k dx^\ell \qquad 2(16)$$

for all

$$2E_{KL} = C_{KL}(X,t) - G_{KL}(X) \qquad 2(17)$$

$$2e_{k\ell} = g_{k\ell}(x) - c_{k\ell}(x,t) \qquad 2(18),$$

which are respectively called *Lagrangian and Eulerian strain tensors.* Our procedure was quite obvious: we transformed the metric tensor $g_{k\ell}$ within ds^2 into the metric tensor C_{KL} from the x^k into the X^K system. This was necessary in order to compare the displacement in the same base system.

Formally we can call

$$c_k(x,t) = G_K(X) \, A^K_k(t) \qquad 2(19)$$

and

$$C_K(X,t) = g_k(x) \, A^k_K(t) \qquad 2(20)$$

the *new base vectors.* The base vectors are dependent on *the position co-ordinates and the time.* They form *four-dimensional moving frames or 4D-Cartan frames.* c_k is called the *Cauchy base vector,*

C^K the *Green base vector*. Finally figure 1 is a brief summary of the geometrical situation .

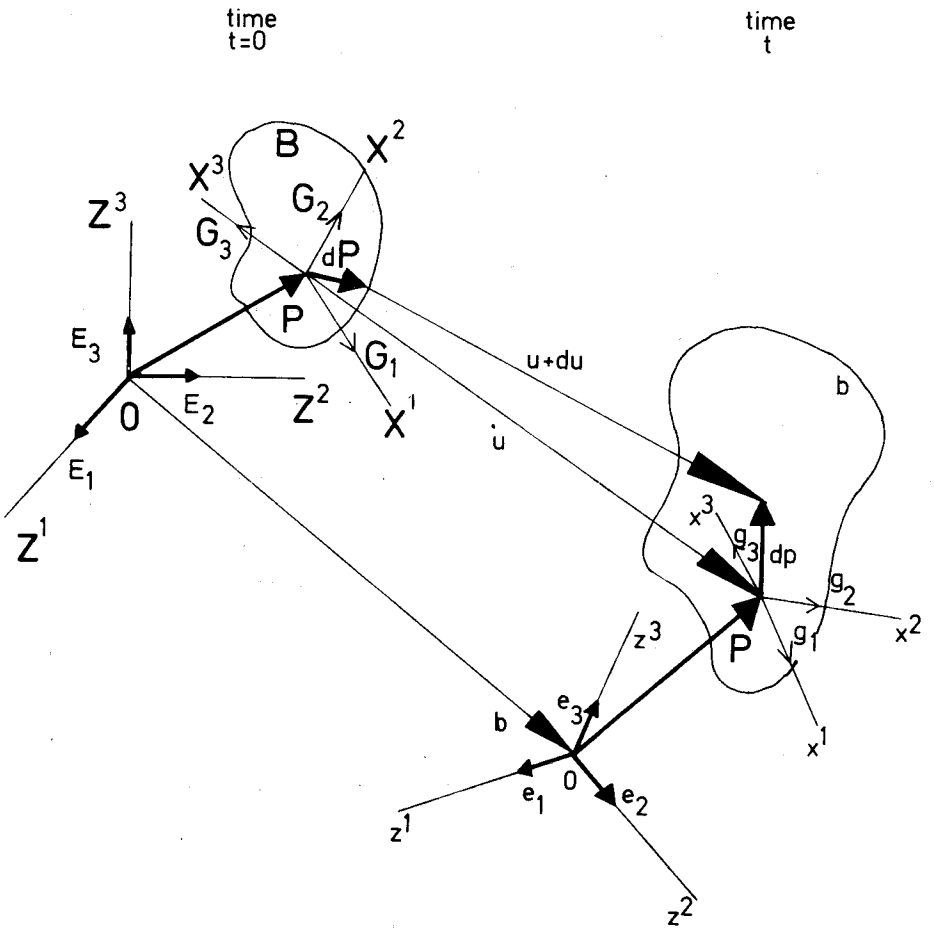

Figure 1. Base Vectors, Displacement Vector and Co-ordinate Systems.

The *displacement vector* is defined as the vector that extends from a material point in the undeformed body to the same material point in the deformed body. Thus

$$u = p - P + b = U^K G_K = u^k g_k \qquad 2(21).$$

If we represent respectively **dp** and **dP** in the 4D-Cartan frames,

$$\mathbf{dp} = C_K \, dX^K = (G_K + U_{M;K} \, G^M) \, dX^K \qquad 2(22)$$

and

$$\mathbf{dP} = c_k \, dx^k = (g_k - u_{m;k} \, g^m) \, dx^k \qquad 2(23),$$

the Lagrangian and Eulerian strain tensors are related to the displacement vector by

$$2E_{KL} = C_{KL} - G_{KL} = U_{K;L} + U_{M;K} U^M{}_{;L} \qquad 2(24)$$

and

$$2e_{k\ell} = g_{k\ell} - c_{k\ell} = u_{\ell;k} - u_{m;k} u^m{}_{;\ell} \qquad 2(25)$$

The semicolon indicates covariant partial differentiation. In the "Small Displacement Theory", the displacement components are considered small. Thus any product of these components and their various gradients may be neglected:

$$2E_{KL} \doteq 2e_{k\ell} \doteq u_{k;\ell} + u_{\ell;k} \qquad 2(26).$$

The differences between U_K and u_k disappear.

In the kinematics of continuous media, time rates of vectors and tensors associated with the material points play an important role. In the determination of the time rate of change of field quantities carried by a material point, one must take into account not only the change at a fixed spatial point (*local change*) but also the change in the field as observed by the particle due solely to its motion (*convective change*). The *material derivative* of an absolute spatial vector $f^k(x,t)$ is defined by

$$\frac{D}{Dt} f^k(x,t) = \frac{\partial f^k}{\partial t} + \frac{\delta f^k}{\delta t} = \frac{\partial f^k}{\partial t} + f^k{}_{;\ell} \frac{dx^\ell}{dt} \qquad 2(27),$$

where the partial time derivative $\partial f^k/\partial t$ is taken with X held constant and the intrinsic derivative $\delta f^k/\delta t$ with t held constant.

In the experimental determination of geometrical and physical properties of the Earth, it is necessary to know how the motion of the observer will affect the measurements. It is evident that for those properties that are independent of the motion of the observer, measurements made in one frame of reference are sufficient to determine their values once and for all.

In the formulation of physical laws, it is desirable to introduce quantities which are independent of the observer or the frame of reference. Such quantities are called *objective*. For example, the location of a point will appear different to observers located at different places, and therefore is not objective. Similarly the velocity of a point will appear to be different to observers moving with respect to each other. Hence again it is not objective. On the other hand, distances and angles are objective quantities since they are independent of the frame of reference.

Attempts to secure the invariance of physical laws of motion from the observer have produced one of the great triumphs of twentieth century physics. Newton's laws of motion have long been known to be valid only in a special frame of reference, the *inertial or Galilean* reference frame. Attempts to free the principles of classical mechanics from the motion of an observer were resolved by A. Einstein in his general theory of relativity, by rejecting these principles altogether and denying an objective meaning for the concept of time and distance.

While we wish to stay in the domain of classical mechanics, we will find that in the description of materials and dynamic processes, the axiom of objectivity plays a central role. To formulate these physically evident facts, let us consider a point x in a reference frame F. In another frame of reference F^1 this point will appear as x^1. The relation between x and x^1 must be such that the distance and the angle are preserved. The most general transformation of space and time that satisfy these conditions are of the form

$$x^1 = Ax + b, \qquad t^1 = t - a \qquad 2(28),$$

where A(t) is an arbitrary real valued non-singular orthogonal matrix, b(t) is an arbitrary point, and a is a constant. Both A and b are continuously differentiable functions of time t alone. The orthogonality condition for the matrix A requires that

$$\mathbf{A}\,\mathbf{A}^T = \mathbf{A}^T\mathbf{A} = \mathbf{I} \qquad 2(29),$$

where $\mathbf{A}^T$ denotes the transposed $\mathbf{A}$ and $\mathbf{I}$ the unit matrix. Suppose $\mathbf{x} = \mathbf{x}(X,t)$ represents the motion of the body B. Then

$$\mathbf{x}^1(X,t^1) = \mathbf{A}(t)\,\mathbf{x}(X,t) + \mathbf{b}(t) \qquad 2(30)$$

indicates that for $t = t^1$, the two frames F and F^1 may move with respect to each other in an arbitrary rigid motion. In rectangular co-ordinates $\mathbf{A}(t)$ for det A = 1 and b(t) represent, respectively, the rotation and the translation of one frame with respect to the other; they behave like moving frames or 4D-Cartan frames.

We have to note that for quantities which are independent of time, objectivity does not come into play. For time dependent quantities, however, the situation is different. If $\mathbf{e}$ is a vector in an inertial frame, it will appear in another frame prime as

$$\mathbf{e}^1 = \mathbf{A}\,\mathbf{e} \qquad 2(31),$$

where $\mathbf{A}$ is a function of time. Because of equations (28),

$$\Omega^* = \frac{DA}{Dt}\,A^T \qquad 2(32)$$

is antisymmetric, since

$$\Omega^* + \Omega^{*T} = \frac{DA}{Dt}\,A^T + A\,\frac{DA^T}{Dt} = \frac{D}{Dt}(A\,A^T) = 0 \qquad 2(33).$$

The dual, Ω, of the matrix Ω^* is a vector, related by

$$\Omega^*_{ij} = \delta_{ij}{}^{k}\,\Omega_k, \qquad \Omega_i = \frac{1}{2}\,\delta_i{}^{jk}\,\Omega^*_{jk} \qquad 2(34)$$

$\delta_{ij}{}^{k}$ denotes the generalized Kronecker symbol, in this case the Levi-Civita symbol. We differentiate (31).

$$\frac{De}{Dt} = \frac{DA^T}{Dt}\,e^1 + A^T\,\frac{De^1}{Dt} \qquad 2(35).$$

It is our aim to resolve the equation along the instantaneous co-ordinate axes of the moving frame.

$$A\,\frac{De}{Dt} = -\,\Omega^*\,(Ae) + \frac{D}{Dt}(Ae) \qquad 2(36).$$

Thus the "velocity" vector is not objective.

3. The Virial Equations of the Various Orders in 4D-Cartan Frames

A technique very much in vogue for treating the integro-differential equations of physical geodesy is to take the moments of the equations concerned. The moment equations have the advantage of allowing simple physical interpretations. The virial method as developed in the context, is mainly the method of moments applied to the solution of rigid, hydrodynamical and elastic problems in which the gravitational field of the matter is taken into account. If we apply the virial method to the equations of motion, we must involve the moments of the distribution of density, stress tensor, for example, pressure, velocity, and gravitational potential.

(a). Let us consider a distribution of mass in a volume v. The frame of reference is for a moment fixed at the centre of mass. Then the choice of the reference frame requires

$$I = \int_v dX\ \rho(X)\ |X|^2 \qquad 3(1),$$

$$I_i = \int_v dX\ \rho(X)\ x_i = 0 \qquad 3(2),$$

$$I_{ij} = \int_v dX\ \rho(X)\ x_i\ x_j \qquad 3(3),$$

and

$$I_{ijk\ldots} = \int_v dX\ \rho(X)\ x_i\ x_j\ x_k \ldots \qquad 3(4),$$

where $\rho(X)$ is the density at the point X. I is the moment of inertia, I_i defining the origin of the mass centre, I_{ij} the moment of inertia tensor.

(b) The prevailing distribution of stresses σ_{ij} similarly leads to a consideration of the moments.

$$\Sigma_{ij} = \int_v dX\ \sigma_{ij} \qquad 3(5),$$

$$\Sigma_{ijk} = \int_v dX\ \sigma_{ij}\ x_k = \int dX\ \sigma_{ijk} \qquad 3(6),$$

and

$$\Sigma_{ijk\ell\ldots} = \int_v dX\ \sigma_{ij}\ x_k x_\ell \ldots. \qquad 3(7),$$

and for a distribution of isotropic pressure $\sigma_{ij} = -p\,\delta_{ij}$

$$\Pi = \int_v dX\ p \qquad 3(8),$$

$$\Pi_i = \int_v dX\ p\ x_i \qquad 3(9)$$

and

$$\Pi_{ij..} = \int_v dX\ p\ x_i\ x_j \ldots.. \qquad 3(10).$$

(c) For a description of the macroscopic motion, we have to refer to the total kinetic energy of the motions in the system.

$$T = \frac{1}{2}\int_v dX\ \rho(X)\ |V|^2 \qquad 3(11),$$

$$T_{ij..} = \frac{1}{2}\int_v dX\ \rho(X)\ v_i v_j \ldots. \qquad 3(12),$$

$$T_{ij|k} = \frac{1}{2}\int_v dX\ \rho(X)\ v_i v_j x_k \qquad 3(13),$$

and

$$T_{ij|k\ell..} = \frac{1}{2}\int_v d\mathbf{X}\ \rho(\mathbf{X})\ v_i v_j x_k x_\ell .. \qquad 3(14),$$

where $|\mathbf{V}|^2 = v_1^2 + v_2^2 + v_3^2$ is the square of the velocity of a material point at $\mathbf{X}$. T_{ij} is the kinetic energy tensor.

(d) The gravitational effect at a point x, due to a distribution of matter with density $\rho(\mathbf{X})$, is determined by the Newtonian potential.

$$V(\mathbf{X}) = G\int_v d\mathbf{X}^1 \quad \frac{\rho(\mathbf{X}^1)}{|\mathbf{X} - \mathbf{X}^1|} \qquad 3(15)$$

and

$$V_{ij}(\mathbf{X}) = G\int_v d\mathbf{X}^1\ \rho(\mathbf{X}^1)\ \frac{(x_i - x_i^1)(x_j - x_j^1)}{|x - x^1|^3} \qquad 3(16).$$

G denotes the constant of gravitation. Associated with the gravitational potential is the potential energy.

$$W = -\frac{1}{2}\int_v d\mathbf{X}\ \rho(\mathbf{X})\ V(\mathbf{X}) \qquad 3(17)$$

and

$$W_{ij} = -\frac{1}{2}\int_v d\mathbf{X}\ \rho(\mathbf{X})\ V_{ij}(\mathbf{X}) \qquad 3(18).$$

(e) We consider a continuous medium of material points described in terms of a density $\rho(\mathbf{X},t)$ and a stress $\sigma_{ij}(\mathbf{X},t)$. Further we suppose that beside the surface force, the only volume force to which the body motions are subject is that derived from its own gravitation. Under these assumptions, the dynamical equation governing the motions, *referred to an inertial frame of reference*, is given by

$$\rho\frac{D}{Dt}v_i = \partial_j \sigma_{ij} + \rho\,\partial_i V \qquad 3(19),$$

where following equation 2(27),

$$\frac{D}{Dt} = \frac{\partial}{\partial t} + v_j\,\partial_j \qquad 3(20)$$

is the material derivative. The virial equations of the various orders are now obtained by simply multiplying the basic dynamical equation, successively by 1, x_j, x_{jk}, $x_j x_k x_\ell$, etc, and integrating over the entire volume v instantaneously occupied by the body.

(f) *The Equations of the First Order*

The equations of the first order are obtained by integrating equation 3(19) over the instantaneous volume V occupied by the body.

$$\frac{D}{Dt}\int_v d\mathbf{X}\ \rho\ v_i = \int_v d\mathbf{X}\ \frac{\partial}{\partial x_j}\sigma_{ij} + \int_V d\mathbf{X}\ \rho\ \frac{\partial V}{\partial x_i} \qquad 3(21),$$

and

$$\frac{D}{Dt}\int_v d\mathbf{X}\ \rho(\mathbf{X},t) = \frac{DM}{Dt} = 0 \qquad 3(22)$$

especially the *local* condition $D\rho/Dt = 0$.

The volume integral $\int_V dx\ \partial_j\ \sigma_{ij}$ can be transformed by the Gaussian integral therein into a surface integral

$$\int_V dX \quad \partial_j \sigma_{ij} \quad = \int_s ds_j \quad \sigma_{ij} \quad = \int_s ds \; n_j \; \sigma_{ij} \qquad 3(23)$$

s denotes the *free surface* bounding the volume v and $ds_j = n_j\, ds$ an element of this surface. n_j is the surface normal vector.

Due to the condition that the normal component of the stress must vanish on a *free boundary*, this surface integral must vanish. By equation 3(15), the second integral in equation 3(21) results zero too, on account of the antisymmetry of the integral in X and X^1.

$$\int_V dX \quad \rho \frac{\partial v}{\partial x_i} \quad = \quad - \quad G \int_V dX \int_V dX^1 \rho(X) \; \rho(X^1) \quad \frac{x_i - x_i^1}{|X - X'|^3} \quad = 0 \qquad 3(24).$$

Thus we are left with the fundamental result

$$\frac{D}{Dt} \int_V dX \; \rho \; v_i \quad = \quad \frac{D^2}{Dt^2} \int_V dX \; \rho \; x_i \quad = \quad \frac{D^2}{Dt^2} I_i \quad = 0 \qquad 3(25)$$

expressing the *uniform motion of the centre of mass*.

(g) *The Equations of the Second Order*

We multiply equation 3(13) by x_j and integrate over the deformed volume v

$$\int_V dX \; \rho \; \frac{Dv_i}{Dt} \; x_j = \int_V dX \; \rho \left\{ \frac{D}{Dt}(v_i x_j) - v_i v_j \right\} \quad = \quad \frac{D}{Dt} \int_V dX \; \rho \; v_i x_j - 2T_{ij}$$

$$= \int_V dX \; (\partial_k \sigma_{ik}) x_j \quad + \int_V dX \; \rho \; x_j \partial_i V \quad = \quad \int_V dX \; \partial_k \sigma_{ijk} - \sum_{ij} + W_{ij} \qquad 3(26).$$

Now we understand that σ_{ijk} are the components of *couple stress* in the deformed state. We note that we have written for $(\partial_k \sigma_{ik}) x_j = \partial_k (\sigma_{ik} x_j) - \sigma_{ik} \partial_k x_j = \partial_k (\sigma_{ijk}) - \sigma_{ij}$. Finally we obtain from equation 3(26) the basic equation 3(27)

$$\frac{D}{Dt} \int_V dX \; \rho \; v_i x_j \quad = \quad 2T_{ij} \quad + \quad S_{ij} - \sum_{ij} + W_{ij} \qquad 3(27).$$

Of course, $\int_V dX \; \partial_k \sigma_{ijk} = \int_s ds \; n_k \sigma_{ijk} = S_{ij}$ by the Gaussian identity. Let us specialize for a moment that we have

1. no plastic effects : $\sigma_{ij} = \sigma_{ji}$; and
2. no couple stresses : $\sigma_{ijk} = 0$.

Then

$$\frac{1}{2} \; \frac{D}{Dt} \int_V dX \; \rho \; (v_i x_j - v_j x_i) \quad = \quad 0 \qquad 3(28)$$

and

$$\frac{1}{2} \; \frac{D}{Dt} \int_V dX \; \rho \; (v_i x_j + v_j x_i) \quad = \quad \frac{1}{2} \frac{D^2}{Dt^2} \int_V dX \quad \rho \; x_i x_j = \frac{1}{2} \frac{D^2 I_{ij}}{Dt^2} \qquad 3(29).$$

Hence we must have

$$\frac{1}{2} \; \frac{D^2}{Dt^2} I_{ij} \quad = \quad 2T_{ij} \quad + W_{ij} \quad - \quad \sum_{ij} \qquad 3(30).$$

(h) *The Equations of Higher Order*

Up to now the reader will be familiar with the virial method. For higher order virial equations, we have to split

$$\int_v dx\ \rho\ \frac{Dv_i}{Dt}\ x_j x_k x_\ell \cdots\cdots \qquad 3(31)$$

by

$$\int_v dx\ \ \rho\{\frac{D}{Dt}(v_i x_j x_k x_\ell \cdots) - (v_i v_j x_k x_\ell \cdots) - (v_i x_j v_k x_\ell \cdots\cdots) - \cdots\cdots\ \} \qquad 3(32).$$

For us, the virial equations in four dimensional moving frames are now most important.

(i) The Second Order Virial Equations in a Moving Frame

From physics it is well known that the virial equations - up to the second order identical with the *first and second laws of motion of Cauchy* - are not objective, but the couple stress tensor is! We apply here only the result of section 2 that

$$\mathbf{A}\frac{D\mathbf{v}}{Dt} = -\Omega^*(\mathbf{Av}) + \frac{D}{Dt}(\mathbf{Av}) \qquad 3(33)$$

for any vector $\mathbf{v}$. Let us denote

$$\mathbf{V} = \mathbf{A}\frac{D\mathbf{x}}{Dt}, \qquad \mathbf{v} = \frac{D\mathbf{x}}{Dt} \qquad 3(34);$$

the velocities in the inertial frame resolved along the instantaneous axes of the moving frame and with respect to an observer at rest in the moving frame, respectively, we can write

$$\mathbf{A}\frac{D\mathbf{x}}{Dt} = \mathbf{V} = \mathbf{v} - \Omega^*\mathbf{x} \qquad 3(35)$$

and

$$\mathbf{A}\frac{D^2\mathbf{x}}{Dt^2} = \frac{D\mathbf{V}}{Dt} = -\Omega^*\mathbf{V} \qquad 3(36).$$

Our basic dynamical equation can therefore be re-written in the form

$$\rho\ \frac{DV_i}{Dt} - \rho\ \Omega^*_{ij}\ V_j = \partial_j\sigma_{ij} + \rho\ \partial_i V \qquad 3(37).$$

To obtain the second order virial equations in a moving frame, we have only to multiply equation 3(37) by the co-ordinates x_j of the deformed state and integrate over the volume v occupied by the material body.

$$\frac{D}{Dt}\int_v dx\ \rho\ V_i x_j = \int_v dx\ \rho\ V_i v_j + \int_v dx\ \rho\ \Omega^*_{im} V_m x_j + S_{ij} - \Sigma_{ij} + W_{ij} \qquad 3(38).$$

Finally we express V(v).

$$\frac{D}{Dt}\int_v dx\,\rho\,v_i x_j - \frac{D}{Dt}\int_v dx\ \rho\ \Omega^*_{im}x_m x_j = \int_v dx\ \rho\ v_i v_j + \int_v dx\ \rho\ \Omega^*_{im}(v_m x_j - v_j x_m) - \int_v dx\ \rho\ \Omega^*_{im}\Omega^*_{m\ell}x_\ell x_j + S_{ij} - \Sigma_{ij} + W_{ij} \qquad 3(39),$$

or alternatively

$$\frac{D}{Dt}\int_V dX\,\rho\, v_i x_j - \frac{D}{Dt}(\Omega^*_{im} I_{mj}) = 2T_{ij} + S_{ij} - \Sigma_{ij} + W_{ij} - \Omega^*_{ik}\Omega^*_{k\ell} I_{\ell j} + \int_V dx\,\rho\,\Omega^*_{im}(v_m x_j - v_j x_m) \qquad 3(40)$$

Why is this equation so important? As an equation of the type of the moment of the momentum, it balances for a general body of rigid - liquid - elastic - plastic type the different influences. We like to point out that this equation even includes couple stress and dislocations. In the next chapters we will present examples for body displacements of rigid, hydrostatic and elastic type. The inclusion of couple stress is under the influence of magnetohydrodynamical effects, essential.

4. Example 1: Rigid Body Displacement

Let us assume $ds^2 = dS^2$, that is, a rigid body displacement, with no stress $\sigma_{ij} = 0$, no couple stress $\sigma_{ijk} = 0$, $\frac{D}{Dt}\rho = 0$, $v_i = 0$. We apply the second order virial equations 3(40) in a moving frame.

$$-\left(\frac{D}{Dt}\Omega^*_{im}\right) I_{mj} + \Omega^*_{ik}\Omega^*_{k\ell} I_{\ell j} = W_{ij} \qquad 4(1).$$

Thus we have found the classical Eulerian dynamical equation for a rigid body in the form of a second rank tensor formula. The dual vector equation is a result of "antisymmetrization"

$$0 = \delta_{ijk} W_{jk} = -\delta_{ijk}\left(\frac{D}{Dt}\Omega_{jm}\right) I_{mk} + \delta_{ijk}\Omega_{j\ell}\Omega_{\ell m} I_{mk} \qquad 4(2).$$

W_{ij} is symmetric, therefore $\delta_{ijk} W_{jk} = 0$ in our Cartesian notation. Of course equation 2(34) holds:

$$I_{ij}\frac{D\Omega_j}{Dt} + \delta_{ijk}\Omega_j\Omega_\ell I_{k\ell} = 0 \qquad 4(3).$$

We note that $\delta_{ijk}\delta_{pqk} = \delta_{ip}\delta_{jq} - \delta_{iq}\delta_{jp}$. It is important that for a self-gravitating body under no outer moments, the vector equation of the moment is balanced! If we call A, B and C the eigenvalues along the eigen vectors of I_{ij}, we arrive at the familar formula

$$\left.\begin{aligned} A\frac{D\Omega_1}{Dt} - (B - C)\Omega_2\Omega_3 &= 0 \\ B\frac{D\Omega_2}{Dt} - (C - A)\Omega_3\Omega_1 &= 0 \\ C\frac{D\Omega_3}{Dt} - (A - B)\Omega_1\Omega_2 &= 0 \end{aligned}\right\} \qquad 4(4).$$

In the case we have other volume couples, we will find an inhomogeneous system! For a symmetric body, A = B; we will study the displacement in more detail:

$$C \frac{D\Omega_3}{Dt} = 0, \qquad \Omega_3 = \Omega_{30} = \text{const.} \tag{4(5)}$$

$$A \frac{D\Omega_1}{Dt} - (A - C)\, \Omega_{30}\, \Omega_2 = 0 \tag{4(6)}$$

and

$$A \frac{D\Omega_2}{Dt} + (A - C)\, \Omega_{30}\, \Omega_1 = 0 \tag{4(7)}$$

We start with $\Omega_1 = \Omega_{10} \sin \delta t$, $\Omega_2 = \Omega_{10} \cos \delta t$, and

$$\delta = \frac{A - C}{A}\, \Omega_{30} = \left(1 - \frac{C}{A}\right) \Omega_{30} \tag{4(8)}$$

The precession frequency δ is periodical with

$$\boxed{T_p = 2\pi\delta^{-1} = \frac{2\pi A}{(A - C)\Omega_{30}}} \tag{4(9)}$$

With the dynamical parameters A, C, Ω_{30} of the Earth we find $T_p = 10$ months, which differs from the measured Chandler period of 14 months. Elastic-plastic effects cause this defect.

5. Example 2: Hydrostatic Body Displacement of Maclaurin Type

Let us assume $ds^2 \neq dS^2$ for a liquid body, that is the stress is isotropic by $\sigma_{ij} = - p\, \sigma_{ij}$, no couple stress $\sigma_{ijk} = 0$, $s_{ij} = 0$, $\sum_{ij} = - \Pi\, \delta_{ij}$, $D\Omega/Dt = 0$.

We apply the second order virial equations 3(40) in this uniformly rotating frame.

$$2T_{ij} + W_{ij} + \Omega^2 I_{ij} - \Omega_i\, \Omega_k\, I_{kj} + \delta_{ij}\, \Pi + 2\delta_{i\ell m}\, \Omega_m \int_V \mathbf{dx}\, \rho\, u_\ell\, x_j = \frac{D}{Dt} \int \mathbf{dx}\, \rho\, v_i\, x_j \tag{5(1)}$$

Under static conditions when there are *no relative motions*, in the rotating frame considered, and which are of interest, $- v_i = 0$ - it is convenient to choose the x_3 axis to be along the direction of the rotation vetor Ω which gives

$$W_{ij} + \Omega^2 (I_{ij} - \delta_{i3} I_{3j}) = - \delta_{ij}\, \Pi \tag{5(2)}$$

The equilibrium figures of *Maclaurin spheroidal type* represent the solution of equation 5(2) when

1. the configuration is of uniform density; and
2. the rotational axis is further assumed to be an axis of symmetry:

$$W_{11} + \Omega^2 I_{11} = W_{33} = - \delta_{ij}\, \Pi \tag{5(3)}$$

$$W_{11} = W_{22} \tag{5(4)}$$

and

$$I_{11} = I_{22} \tag{5(5)}$$

Let us have a look for solutions of the ellipsoidal type. From classical potential theory we find for the energy potential tensor W_{ij} for a homogeneous ellipsoid

$$\frac{W_{ij}}{\pi G \rho} = -2A_i\, I_{ij} \tag{5(6)}$$

where the moment of inertia tensor is due to

$$I_{ij} = \frac{1}{5} M a_i^2 \delta_{ij} \qquad 5(7)$$

and the mass

$$M = \frac{4}{3} \Pi a_1 a_2 a_3 \qquad 5(8).$$

a_i are the eigenvalues in the eigen directions of an ellipsoidal canonical two-form. The index symbols are defined by

$$A_i = a_1 a_2 a_3 \int_0^\infty du\left[(a_1^2 + u)(a_2^2 + u)(a_3^2 + u)\right)^{-\frac{1}{2}} \qquad 5(9).$$

Inserting for W_{11} and W_{33} gives

$$-2(\pi G\rho)A_1 I_{11} + \Omega^2 I_{11} = -2(\pi G\rho)A_3 I_{33} \qquad 5(10)$$

and

$$\frac{\Omega^2}{\pi G\rho} = 2\left(A_2 - \frac{a_3^2}{a_1^2} A_3\right) \qquad 5(11).$$

If $a_1 = a_2 > a_3$, the integrals defining the A_i's are elementary:

$$A_1 = A_2 = \frac{(1 - e^2)}{e^3} \sin^{-1} e - \frac{1 - e^2}{e^2} \qquad 5(12)$$

and

$$A_3 = \frac{2}{e^2} - \frac{2(1 - e^2)^{\frac{1}{2}}}{e^3} \sin^{-1} e \qquad 5(13),$$

where $e^2 = 1 - a_3^2/a_1^2$, defines the eccentricity of the meridional sections. Substituting for A_1 and A_3 in equation 5(11), we have Maclaurin's formula

$$\frac{\Omega^2}{\pi G\rho} = \frac{2(1 - e)^{\frac{1}{2}}}{e^3} (3 - 2e^2) \sin^{-1} e - \frac{6}{a^2}(1 - e^2) \qquad 5(14),$$

plotted in figure 2.

6. Example 3: Elastic Body Displacement of LOD and Wobble Type

Let us assume $ds^2 \neq dS^2$ for an elastic body, especially within the "Small Displacement Theory" of isotropic type, i.e.,

$$\sigma_{ij} = \lambda(\mathrm{tr}\, e_{k\ell})\, \delta_{ij} + 2\mu\, e_{ij} \qquad 6(1),$$

where λ and μ are Lame's constants, with no couple stress $\sigma_{ijk} = 0$, $S_{ij} = 0$. We apply the second order virial equations 3(40) in a moving frame,

$$\frac{D}{Dt}\int_v dx\, \rho\, v_i x_j - \frac{D}{Dt}(\Omega^*_{im} I_{mj}) = 2T_{ij} - \sum_{ij} + W_{ij} - \Omega^*_{ik}\Omega^*_{k\ell} I_{\ell j} + \int_v dx\, \rho\, \Omega^*_{im}(v_m x_j - v_j x_m) \qquad 6(2)$$

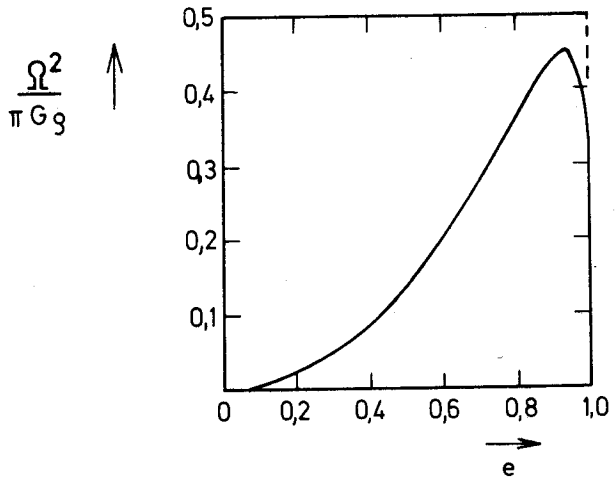

Figure 2. The Square of the Angular Velocity in Units of $\pi G\rho$ along the Maclaurin Sequences

For the data of the Earth: mean density $\rho = 5.514$ g cm^{-3}, $G = 6.674 \times 10^{-8}$ cm^3 g^{-1} sec^{-2}, and $\Omega = 7.292 \times 10^{-5}$ sec^{-1}, the value of $(\Omega^2/\pi G\rho)$ is about 0.025, not too far away from an eccentricity of about 0.00672.

generalizing the Euler - Liouville equations for a deformable body. The global stress tensor is now due to

$$\sum_{ij} = \int_V dX\ \sigma_{ij} = \delta_{ij} \int_V dX\ \lambda(\mathrm{tr}\ e_{k\ell}) + 2\int_V dX\ \mu\ e_{ij} \qquad 6(3)$$

in general, for inhomogeneous elastic bodies, and the Lame's constants λ and μ are functions of the position within the body. Inserting from equation 2(25) of the displacement vector leads to

$$2e_{k\ell} = u_{k;\ell} + u_{\ell;k}, \qquad \mathrm{tr}\ e_{k\ell} = \frac{1}{2}(\partial_1 u_1 + \partial_2 u_2 + \partial_3 u_3) \qquad 6(4).$$

The structure of equation 6(2) is very similar to the structure of the Eulerian dynamical equations for a rigid body. This will be quite obvious if we rewrite equation 6(2)

$$\frac{D}{Dt}\left(-\Omega^*_{im} I_{mj} + \int_V dX\ \rho\ v_i x_j\right) + \int_V dX\ \rho\ \Omega^*_{ik}\left(\Omega^*_{k\ell} I_{\ell j}/M - v_k x_j + v_j x_k\right) = W_{ij} + 2T_{ij} - \sum_{ij} \qquad 6(5).$$

It is very interesting that in the dual vector equation of 5(2), the right hand side quantities W_{ij}, T_{ij}, $\sum_{ij}$ vanish because of their symmetry. Therefore we have to work with equation 6(2)! Of course, this statement is true for the "liquid" equation 5(1), too.

The well known procedure of perturbation theory leads simply to the classical LOD and wobble analysis, but in our case in terms of Lame's constants, avoiding the concept of Love numbers. Finally, if we are only interested in the static situation we will have no relative motions:

$$-\frac{D}{Dt}(\Omega^*_{im} I_{mj}) = -\sum_{ij} + W_{ij} - \Omega^*_{ik}\,\Omega_{k\ell}\,I_{\ell j} \qquad 6(6).$$

For more details of how to solve equation 6(2), the reader is referred to MUNK & MACDONALD (1960, p.38 et seq.).

7. References

BOCCHIO, F. 1970. Su Alcune Applicazioni de Interesse Geodetico delle Connessioni non Simmitriche. *Acad.Naz.Linc.*, Rome,p.343.

CHANDRASEKHAR, S. 1969. *Ellipsoidal Figures of Equilibrium.* Yale University Press, New Haven Conn.

DE WIT, R. 1967. Differential Geometry of nonlinear Continuum Theory of Dislocations. In (KROENER, E ed.) *IUTAM - Symposium on "The Generalized Cosserat Continuum and the Continuum Theory of Dislocations with Applications", Freudenstadt/Stuttgart 1967.* Springer-Verlag, Berlin.

GRAFAREND, E. 1971. The Object of Anholonomity and a Generalized Riemannian Geometry for Geodesy. *Boll.Geof.Teor.Appl.* 13,241.

GRAFAREND, E. 1972. Three Dimensional Geodesy and Gravity Gradients. *Rep.* 174,Dept. of Geodetic Science,The Ohio State University,Columbus Ohio.

GRAFAREND, E. 1973a. Attempts for a Unified Theory of Geodesy. *Boll.geodesia e Scienze Affini* 32, 231.

GRAFAREND, E. 1973b. Gravity Gradients and Three Dimensional Net Adjustments without Ellipsoidal Reference. *Rep.* 202,Dept. of Geodetic Science,The Ohio State University,Columbus Ohio.

GRAFAREND, E. 1973c. *Cartan Frames and a Foundation of Physical Geodesy.* International Summer School in the Mountains, Ramsau Austria.

GRAFAREND, E & SCHAFFRIN, B 1973. Unbiased Free Net Adjustment. *Surv.Rev.* (in press).

GROSSMAN, N. 1973. Marussi Theorem and Holonomic Measurables. *J.geophys.Res.* (in press)

HOTINE, M. 1969. Mathematical Geodesy. *ESSA Monograph* 2,Washington DC.

KROENER, E. 1960. *Arch.Rat.mech.Anal.* 4,273.

MARUSSI, A. 1949. Fondements de Geometrie Differentielle Absolue du Champ Potential Terrestre. *Bull.géodes.* 14,411.

MUNK, W.H. & MACDONALD, G.J.F. 1960. *The Rotation of the Earth.* Cambridge University Press.

SCHOUTEN, J.A. 1954. *Ricci-Calculus.* Berlin.

8. Discussion

LAMBECK: I am a little disturbed by your dislike for the Love numbers. It is generally recognized that they offer very convenient ways of describing integral effects of the Earth's elastic (and anelastic) properties, in particular, when the details of the distribution of the elastic parameters within the Earth are not adequately known. In this sense they act as transfer parameters between observations and theory. Once observed, they then have to be interpreted in terms of the physics of the Earth. I agree that due to the multiplicity of types of Love numbers, this question of interpretation is most difficult.

GRAFAREND: This approach is rigorous if you accept stress-strain relationships of this kind. The problem of Love numbers is that they are really intuitive, and specialists introduce concepts like non-linear Love numbers. The original paper of Love gives a number of definitions of Love numbers. The problem of Love numbers is that they depend on the model being used.

KAULA: The Love numbers are rigorous for spherical Earth models. For a Maxwell rheology you can use complex Love numbers. More realistic rheologies may lead to more complicated Love operators.

GRAFAREND: Right. If one had spherical symmetry the problem would be solved. Why is no one working with the classical approach used in physics where you have continuum mechanics and where, for example, you refer to elasticity, you have Lamé's constants? Everyone in seismology is working with elastic constants. I don't see too many reasons why we need Love numbers for this purpose.

LAMBECK: You have oversimplified the problem. In seismology one measures directly the Lame parameters as a function of position and Love numbers do not enter into the problem. For tidal loading and rotational studies, however, one must also consider oceanic, atmospheric and liquid core effects and these cannot usually be treated in the same way as can the elastic mantle. In particular, these fluid effects can differ depending on the problem. For example, whether or not the axis of rotation is variable or whether the forcing function has a frequency close to the free oscillation of the fluid part. Your approach is an interesting one but I do not see how you can include these various effects with any more certitude than one can interpret the Love numbers now.

WHITTEN (Chairman): GRAFAREND told us he has worked two years on this paper. We should not expect to grasp its full meaning in a few minutes. Unfortunately we have to move on to the next paper .....

MORGAN, P.
Division of National Mapping
Department of Minerals & Energy
Canberra ACT 2600
Australia

Proc. Symposium on Earth's Gravitational Field & Secular Variations in Position (1973), 660-673.

CRUSTAL VELOCITY AND STRAIN

ABSTRACT

Historically geodesists have measured displacements relative to an assumed or known fixed position and made these observations available for the computation of other geodetic/geophysical parameters. Strain analysis performed in such a manner is usually accomplished in a Lagrangian system of co-ordinates and results in numerous approximations, many of which break down at, or close by, yield point which accompanies earthquakes.

A more powerful approach appears to be via the determination of velocity fields. In this approach a particle or point is tracked through the prevailing velocity field, which may not be constant with time. The system of co-ordinates used in such an analysis is Eulerian and has the immediate advantage that the differential of the velocity field, the Jacobian, contains both the rotationally symmetric part and anti-symmetric part, without approximation of the strain rate tensor.

A number of methods of determining the strain rate tensor from observations over meso and maro areas are developed with the view of determining and monitoring the state of strain of an area, as it is changes of state that appear to be most important. Continental motion most probably can be viewed as a continuous process with peaks in state of strain which must be relieved by violent crustal motions.

1. Preamble

The historical role of geodesy, the study of the size and shape of the Earth, was directed towards the attainment of national, and just lately global, networks which adequately describe, for most mapping purposes, the parametric relationship between points in such networks as well as the surface on which these points lie. These networks are essential for national mapping programs, communications and the distribution of essential commodities. Having fulfilled these requirements, at least in the so-termed developed sector, geodesy was in danger of having completed its mission just as physics was in the time of Lord Kelvin.

In today's world, geodesy is no longer the simple study of the Earth's size and shape but also of secular changes that take place in its size and shape.

It can be argued that all changes and advancements in the applied sciences, as distinct from the pure sciences, are derived from a basic need or series of such needs. In our present world a basic need is the understanding of volcanic and seismic activity and the possibly interrelated phenomena of polar motion, particularly Chandlerian motion, with the view of predicting such events on a global as well as a local scale.

This paper addresses itself to the gathering and possible interpretation of suitable geodetic observations for investigations into the secular nature of the behaviour of the planet Earth under the

assumption that descriptive parameters are not constant with time, nor are they constant in space.

2. An Introduction to Elastic Theory and Crustal Movement

2.1 The Strain Tensor

Consider a general spatial region over which a geodetic network is laid. The region is initially unstressed and a general point in the area has arbitrarily assigned to it co-ordinates

$$X_p = \begin{pmatrix} x \\ y \\ z \end{pmatrix}_p$$

in the geocentric system. The squared length of a differential element is therefore represented as follows (BORG 1963)

$$d\ell_p^2 = dx^2 + dy^2 + dz^2 = dX_p^T \cdot dX_p \qquad (1).$$

If the area is now subjected to strain such that this general point moves relative to the origin of the system, then its new position, X_1, can be expressed as a function of the old position as follows:

$$X_1 = X_p + \begin{pmatrix} h_1(X_p) \\ h_2(X_p) \\ h_3(X_p) \end{pmatrix} = G(X_p) \qquad (2).$$

The differential element of length must reflect this change and a state of strain is introduced as a result of changes in the differential element. This state of strain is defined as the difference in square length, viz, state of strain, given by

$$\text{State of Strain} = dX_1^T \cdot dX_1 - dX_p^T \cdot dX_p \qquad (3),$$

where the differential element dX_1 can be expressed, by virtue of the above functional dependency, as:

$$dX_1 = J\,dX_p = \begin{pmatrix} \frac{\partial g_1(X_p)}{\partial x_p} & \frac{\partial g_1(X_p)}{\partial y_p} & \frac{\partial g_1(X_p)}{\partial z_p} \\ \frac{\partial g_2(X_p)}{\partial x_p} & \frac{\partial g_2(X_p)}{\partial y_p} & \frac{\partial g_2(X_p)}{\partial z_p} \\ \frac{\partial g_3(X_p)}{\partial x_p} & \frac{\partial g_3(X_p)}{\partial y_p} & \frac{\partial g_3(X_p)}{\partial z_p} \end{pmatrix} \cdot \begin{pmatrix} dx_p \\ dy_p \\ dz_p \end{pmatrix} \qquad (4).$$

It is convention to refer to J as the Jacobian although the more common geodetic nomenclature is the partial differential matrix of the function with respect to the parameters.

Substitution of equation set 4 into equation set 3 yields after simplification:

$$\text{State of Strain} = dX_p^T\,(J^T \cdot J - I)\,dX_p \qquad (5).$$

The important quantity here is $J^T \cdot J - I$, which is directly proportional to the classically defined strain tensor η:

$$\eta = \tfrac{1}{2}(J^T \cdot J - I) \qquad (6)$$

It is important to note that η has been derived without any restrictions and may be used for large strains, as all second order terms are included. In particular it is to be noted that the co-ordinate system is Lagrangian rather than the classical Eulerian system.

Expounding upon the last statement, it has been assumed historically that in equation set 2, there is no essential difference between X_p and X_1 and that all displacements are small linear displacements. That is, the differentials are performed about the new point rather than the old point. In essence this can be interpreted as follows:

> The Eulerian system specifies the conditions at each point in the deformed region whereas the Lagrangian system attempts to follow the motion of a particle, the survey peg, in the deformed region, thereby relating all subsequent positions by functions to the initial position.

Of necessity the changes must be small if the Eulerian system is to be used as second order terms are defined to be zero, that is, the derived tensor η has as its symmetric components those elements which make up the Eulerian rotationally symmetric strain tensor. The non symmetric terms are the second order effects. The diagonal elements of η represent the elongation/contraction of the network while the off-diagonal terms refer specifically to the non-uniform shear deformation to which the region is being subjected.

2.2 The Stress Tensor

When a region is subject to strain (deformation), it is being elongated/contracted or sheared by forces acting on the boundaries or faces of the region. These forces must have resultant forces, which are manifested by deformation. The stress that a region undergoes during the deformation is defined to be equal to the force acting per unit area, i.e.,

$$\text{Stress} = \frac{\partial \text{ Force}}{\partial \text{ Area}} = \frac{\partial F}{\partial A} = \frac{\partial}{\partial A} F \, .$$

Generalizing this definition to three-dimensional forces,

$$F = \begin{pmatrix} F_x \\ F_y \\ F_z \end{pmatrix} \quad \text{and, after considering a multifaced body for which} \quad A = \begin{pmatrix} A_x \\ A_y \\ A_z \end{pmatrix},$$

the following stress tensor is obtained:

$$T = \left(\frac{\partial}{\partial A} \right) \cdot F^T = \begin{pmatrix} \frac{\partial}{\partial A_x} \\ \frac{\partial}{\partial A_y} \\ \frac{\partial}{\partial A_z} \end{pmatrix} \cdot \left(F_x, F_y, F_z \right) \qquad (7),$$

that is,

$$T = \begin{pmatrix} \frac{\partial F}{\partial A_x^x} & \frac{\partial F}{\partial A_x^y} & \frac{\partial F}{\partial A_x^z} \\ \frac{\partial F}{\partial A_y^x} & \frac{\partial F}{\partial A_y^y} & \frac{\partial F}{\partial A_y^z} \\ \frac{\partial F}{\partial A_z^x} & \frac{\partial F}{\partial A_z^y} & \frac{\partial F}{\partial A_z} \end{pmatrix} = \begin{pmatrix} \sigma_x & \tau_{xy} & \tau_{xz} \\ \tau_{yx} & \sigma_y & \tau_{yz} \\ \tau_{zx} & \tau_{zy} & \sigma_z \end{pmatrix} \qquad (8).$$

This strain tensor is symmetric by virtue of the necessary static equilibrium and moment conditions that must hold for differential elements. Consequently it can be resolved into principal components

if necessary. In particular the main diagonal elements represent normal forces while off-diagonal elements represent shearing forces.

2.3 The Strain Rate Tensor

The strain and stress tensors reflect the state existing in a region after an initial epoch at which the region was unstrained. This is a non-recoverable epoch or condition and, since these states may be continually changing, it is also necessary to consider changes in these tensors. That is the secular change of the strain and stress tensors is of great interest in determining the state of the Earth.

Consider only the variation that is the first order differential of the strain tensor, since the stress tensor is related to it by Hooke's law. Then, to first order accuracy, the following holds for equation set 6:

$$\delta\eta = \tfrac{1}{2}[(\delta J^T)\, J + J^T\, (\delta J)] \qquad (9).$$

From equation set 4, it is evident that the basic definition of the Jacobian is

$$J^T = \begin{pmatrix} \frac{\partial}{\partial x} \\ \frac{\partial}{\partial y} \\ \frac{\partial}{\partial z} \end{pmatrix} \cdot G^T(X_p).$$

Under the assumption that the second derivatives are continuous and the variables are independent, then

$$J^T = \begin{pmatrix} \delta\frac{\partial}{\partial x} \\ \delta\frac{\partial}{\partial y} \\ \delta\frac{\partial}{\partial z} \end{pmatrix} \cdot G^T(X_p) = \begin{pmatrix} \frac{\partial}{\partial x} \\ \frac{\partial}{\partial y} \\ \frac{\partial}{\partial z} \end{pmatrix} \cdot \delta G^T(X_p) \qquad (10).$$

By definition $G(X_p)$ is a spatial field of points. At the initial epoch, X_p and X_1 are coincident but the survey point is being subjected to pressure to force a separation. That is, it has velocity and possibly acceleration which may be time dependent.

Now

$$G^T(X_p) = \frac{\partial G^T}{\partial X_p} \cdot \delta X_p + \frac{\partial G^T}{\partial t} \cdot \delta t.$$

From the above definition,

$$\frac{\partial G^T}{\partial X_p} \cdot \delta X_p = 0,$$

and hence

$$G^T(X_p) = \dot{G} \cdot \delta t.$$

Consequently

$$\delta J^T = \begin{pmatrix} \frac{\partial}{\partial x} \\ \frac{\partial}{\partial y} \\ \frac{\partial}{\partial z} \end{pmatrix} \cdot G^T\, \delta t = \dot{J}\, \delta t \qquad (11).$$

Substituting equation set 11 into equation sets 9, and noting that $J = I$ by virtue of the fact that $\begin{bmatrix} h_1(X_p) \\ h_2(X_p) \\ h_3(X_p) \end{bmatrix}$ of equation set 2 must be replaced by $\begin{bmatrix} h_1(t) \\ h_2(t) \\ h_3(t) \end{bmatrix}$, then equation set 9 reduces to the following well known equation which defines the strain rate tensor, also referred to as the rate of deformation matrix:

$$\frac{\delta \eta}{\delta t} = \dot{\eta} = \tfrac{1}{2}(\dot{J}^T + \dot{J}) \qquad (12).$$

Thus at this stage it becomes practical to solve for those forces and/or stresses that control crustal movement, and their secular changes. Elastic theory is outside the scope of these discussions which will now centre on how best to obtain $G(X_p)$. Full discussions on elastic theory have been presented by TIMOSHENKO & GOODIER (1951), LOVE (1920) and SOKOLNIKOFF (1956).

3. The Photogrammetric Model

Using the notation indicated in section 7.2, the well known collinearity condition equation can be expressed as follows:

$$x_p - x_o = - f[M_1(X_p - X_o)/M_3(X_p - X_o)]$$

and

$$y_p - y_o = - f[M_2(X_p - X_o)/M_3(X_p - X_o)] \qquad (13).$$

The augmentation of these equations to accept the velocity concept is conceptually very simple since the following definition can be made:

$$X_1 = X_p + V_p(t)$$

and as a consequence X_1 is substituted in the above for X_p.

The solution of the augmented collinearity condition equations is in accordance with the normal conventions and procedures. In particular it can be expected that some ground survey will have taken place and hence some additional observations on the unknown parameter set will be available. This can be represented as:

$F(L_a^1, X_a) = 0$ for the image space, and $G(L_a^2, X_a) = 0$ for the object space.

This is the classical dual observation set on the same unknown parameters which was fully treated by BROWN (RCA54), except that additional observations are on the unknown object space parameters associated with ground points and not on the camera station and its orientation.

The classical solution of this problem can be expressed as follows, using the notation of UOTILA (1967)

$$\begin{bmatrix} A_1^T(B_1P_1^{-1}B^T)^{-1}A_1 & A_2^T \\ A_2 & -B_2P_2^{-1}B_2^T \end{bmatrix} \cdot \begin{bmatrix} X \\ -K_2 \end{bmatrix} = \begin{bmatrix} -A_1(B_1P_1^{-1}B^T)^{-1}W_1 \\ -W_2 \end{bmatrix} \qquad (14).$$

In an effort to determine the conditions under which a solution can be obtained, it is more instructive to introduce the fixed and/or known points into the model by means of the following conditions:

$$F(L_a^1, X_a) = 0, \qquad G(L_a^2, X_a) = 0, \qquad \text{and} \qquad H(X_a) = 0 \tag{15}$$

The solution of the system is an augmented form of equation set 14:

$$\begin{bmatrix} A_1^T(B_1P_1^{-1}B^T)^{-1}A_1 & A_2^T & C^T \\ A_2 & -B_2P_2^{-1}B_2^T & 0 \\ C & 0 & 0 \end{bmatrix} \cdot \begin{bmatrix} X \\ -K_2 \\ -K_c \end{bmatrix} = \begin{bmatrix} -A_1^T(B_1P_1^{-1}B^T)^{-1}W_1 \\ -W_2 \\ -W_3 \end{bmatrix} \tag{16}$$

where

$$C = \frac{\partial G}{\partial \text{parameter}} .$$

It is to be noted that for observation equation work, B = I, resulting in considerable simplification of the above. The necessary and sufficient condition for solution is:

$$(2n + m) + (p + q) > (2n + m) > (p + q),$$

where
- n is the number of photographic images observed,
- m is the number of ground survey observations,
- p is the number of unknown parameters, and
- q is the number of conditions being impressed.

Unfortunately there is also a stability condition that has to be met if a numerical value is to be obtained. That is, if the p+q sector is ill-determined then this has the effect that in the above equation, the first condition is not satisfied.

A full exposé of methods of handling the analytic photogrammetric problem may be found in the various publications of Brown.

4. The Geodetic Model

The augmentation of geodetic short arc formulae to accommodate velocity terms is similar in theory to that proposed in the photogrammetric model except that the observations cannot be made at a single epoch. Consequently in a dynamic environment the same spatial point cannot be observed at a number of different epochs and allowances must be made for this fact.

The direct problem is normally associated with the determination of the point under observation, P_2, from an initial point P_1 It is characterized in this context by the following relationship:

$$\begin{bmatrix} \phi_2 \\ \lambda_2 \\ A_{21} \end{bmatrix} = F(\phi_1, \dot{\phi}_1, \lambda_1, \dot{\lambda}_1, A_{12}, S, t).$$

The inverse problem is associated with an assumed knowledge of station values and the need to deduce the parameters specifying the separation. It is characterized as follows :

$$\begin{bmatrix} S \\ A_{12} \\ A_{21} \end{bmatrix} = G(\phi_1, \dot{\phi}_1, \lambda_1, \dot{\lambda}_1, \phi_2, \dot{\phi}_2, \lambda_2, \dot{\lambda}_2, t).$$

It is this form which is equivalent to the mathematical model that is normally used in least squares solutions $L_a = F(X_a)$. However it is considered important to derive both cases. The method used follows that developed by CLARK (1963) in proving the Puissant form of the direct and indirect problem.

4.1 The Direct Geodetic Problem

Consider now figure 1, the equivalent sphere polar triangle. The spatial co-ordinates of the two points P_1 and P_2 are functions of time in the aforementioned prescribed manner. Applying the cosine law to the observed triangle P_1-P_2-Pole, (Δ-P_1-P_2-Pole), and simplifying by the application of double angle formulae yields :

$$\sin(\phi_2 + \dot{\phi}_2\Delta t) = \sin(\phi_1 + \dot{\phi}_1\Delta t)\cdot\cos\left(\frac{S}{N_E}\right) + \cos(\phi_1 + \dot{\phi}_1\Delta t)\cdot\sin\left(\frac{S}{N_E}\right)\cos A_{12} \qquad (19).$$

Defining $\phi_2 = \phi_1 + d\phi$, and expanding equation 19 by means of double angle expressions yields:

$$\sin(\phi_1+ \dot{\phi}_2\Delta t)\cdot\cos d\phi + \sin d\phi\cdot\cos(\phi_1+ \dot{\phi}_2\Delta t) = [\sin\phi_1\cdot\cos(\dot{\phi}_1\Delta t) + \sin(\dot{\phi}_1\Delta t)\cdot\cos\phi_1]\cdot\cos\left(\frac{S}{N_E}\right)+$$

$$[\cos\phi_1\cdot\cos(\dot{\phi}_1\Delta t) - \sin\phi_1\cdot\sin(\dot{\phi}_1\Delta t)]\cdot\sin\left(\frac{S}{N_E}\right)\cdot\cos A_{12} \qquad (20).$$

Now the left hand side of equation 20 can be expressed, after trigonometrically expanding the double angles, followed by a power series expansion of all small quantities to the third order and re-arrangement as:

$$\sin\phi_1\cdot\left(1 - \frac{(\dot{\phi}_2\cdot\Delta t)^2}{2} + \frac{\cos\phi_1}{\sin\phi_1}(\dot{\phi}_2\cdot\Delta t)\right) + \cos\phi_1\cdot d\phi\left(1 - \frac{(\dot{\phi}_2\cdot\Delta t)^2}{2} - \frac{\sin\phi_1}{\cos\phi_1}(\dot{\phi}_2\cdot\Delta t)\right) -$$

$$\sin\phi_1\cdot\frac{(d\phi)^2}{2}\left(1 - \frac{(\dot{\phi}_2\cdot\Delta t)^2}{2} + \frac{\cos\phi_1}{\sin\phi_1}(\dot{\phi}_2\cdot\Delta t)\right) - \cos\phi_1\frac{(d\phi)^3}{6}\cdot\left(1 - \frac{(\dot{\phi}_2\cdot\Delta t)^2}{2} - \frac{\sin\phi_1}{\cos\phi_1}(\dot{\phi}_2\cdot\Delta t)\right) \qquad (21).$$

Treating the right hand side of equation 20 in the same manner yields the following:

$$\sin\dot{\phi}_1\cdot\left(1 - \frac{(\dot{\phi}_1\cdot\Delta t)^2}{2} + \frac{\cos\phi_1}{\sin\phi_1}(\dot{\phi}_1\cdot\Delta t)\right) + \frac{S}{N_E}\cdot\cos A_{12}\cdot\cos\phi_1\cdot\left(1 - \frac{(\dot{\phi}_1\cdot\Delta t)^2}{2} - \frac{\sin\phi_1}{\cos\phi_1}(\dot{\phi}_1\cdot\Delta t)\right) -$$

$$\frac{S^2}{2N_E^2}\cdot\sin\phi_1\cdot\left(1 - \frac{(\dot{\phi}_1\cdot\Delta t)^2}{2} + \frac{\cos\phi_1}{\sin\phi_1}(\dot{\phi}_1\cdot\Delta t)\right) - \frac{S^3}{6N_E^3}\cdot\cos\phi_1\cdot\cos A_{12}\cdot\left(1 - \frac{(\dot{\phi}_1\cdot\Delta t)^2}{2} - \frac{\sin\phi_1}{\cos\phi_1}(\dot{\phi}_1\cdot\Delta t)\right) \qquad (22).$$

Now defining

$$1 - \frac{(\dot{\phi}_1\cdot\Delta t)^2}{2} - \frac{\sin\phi_1}{\cos\phi_1}\cdot(\dot{\phi}_1\cdot\Delta t) = I_1 \; ; \qquad 1 - \frac{(\dot{\phi}_2\cdot\Delta t)^2}{2} - \frac{\sin\phi_1}{\cos\phi_1}\cdot(\dot{\phi}_2\cdot\Delta t) = I_2 \; ;$$

$$1 - \frac{(\dot{\phi}_1\cdot\Delta t)^2}{2} + \frac{\sin\phi_1}{\cos\phi_1}\cdot(\dot{\phi}_1\cdot\Delta t) = J_1 \; ; \text{ and } \; 1 - \frac{(\dot{\phi}_2\cdot\Delta t)^2}{2} + \frac{\sin\phi_1}{\cos\phi_1}\cdot(\dot{\phi}_2\cdot\Delta t) = J_2 \qquad (23),$$

and introducing these definitions yields, after re-arrangements the following expression for $d\phi$, the difference in latitude at some standard epoch:

$$d\phi = \tan\phi_1\cdot\frac{J_2}{2I_2}\cdot(d\phi)^2 + \frac{(d\phi)^3}{6} + \frac{S}{N_E}\cdot\cos A_{12}\cdot\frac{I_1}{I_2} - \frac{S^2}{2N_E^2}\cdot\tan\phi_1\cdot\frac{J_1}{J_2} - \frac{S^3}{6N_E^3}\cdot\cos A_{12}\cdot\frac{I_1}{I_2} + \tan\phi_1\frac{J_1 - J_2}{I_2} \qquad (24).$$

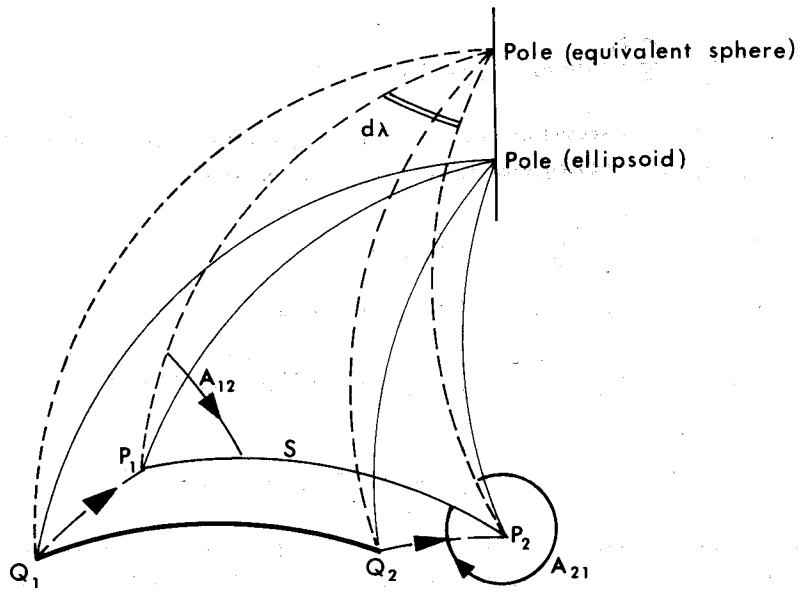

$$P_1 = Q_1 + \begin{bmatrix} \dot{\phi}_1 \cdot \Delta t \\ \dot{\lambda}_1 \cdot \Delta t \end{bmatrix} \qquad P_2 = Q_2 + \begin{bmatrix} \dot{\phi}_2 \cdot \Delta t \\ \dot{\lambda}_2 \cdot \Delta t \end{bmatrix}$$

Figure 1: The Polar Triangles at Observation and Standard Epoch

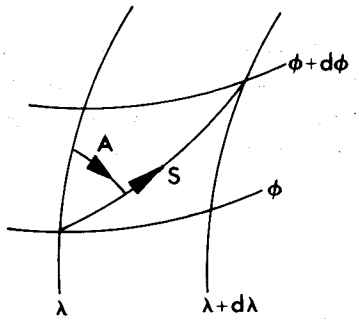

Figure 2: The Differential Figure

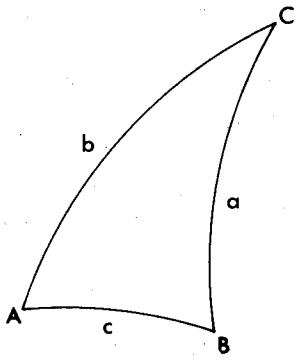

Figure 3: The Spherical Triangle

Consider now the differential geodetic figure - figure 2 - from which the relationship

$$d\phi = \frac{S}{N_E} \cdot \cos A_{12}$$

is derived. When substituted into equation 24, the following relationship is obtained under the additional initial assumption that $I_1 = I_2 = J_1 = J_2 = 1$:

$$d\phi = \frac{S}{N_E} \cdot \cos A_{12} - \frac{S^2}{N_E^2} \cdot \frac{\tan \phi_1}{2} \cdot \sin^2 A_{12} - \frac{S^3}{6N_E^3} \cdot \cos A_{12} \cdot \sin^2 A_{12} \qquad (25).$$

Now neglecting terms higher than second order, since their contribution is less than 5×10^{-6} for a 100 km line, then the following updated expression for $d\phi$ is obtained:

$$d\phi = \frac{S}{N_E} \cdot \cos A_{12} - \frac{S^2}{2N_E^2} \tan \phi_1 \sin^2 A_{12},$$

which is re-substituted into equation 24, yielding after simplification:

$$d\phi = \frac{S}{N_E} \cdot \cos A_{12} \cdot \frac{I_1}{I_2} - \frac{\tan \phi_1}{2} \cdot \frac{S^2}{N_E^2} \cdot \left(\frac{J_1}{I_2} - \frac{J_2}{I_2} \cos^2 A_{12} \right) - \frac{S^3}{6N_E^3} \cdot \cos A_{12} \cdot \left(\frac{I_1}{I_2} - 1 + \sin^2 A_{12} + 3 \sin^2 A_{12} \cdot \tan^2 \phi_1 \cdot \frac{J_2}{I_2} \right) + \tan \phi_1 \cdot \left(\frac{J_1 - J_2}{I_2} \right) \qquad (26).$$

Under the assumption that the velocity field is not too irregular and that we are considering lines less than 100 km long, the definition equation set 23 can be used to simplify equation 26 if $I_1 \sim I_2$ and $J_1 \sim J_2$. Under these assumptions, it reduces to:

$$d\phi = \frac{S}{N_E} \cdot \cos A_{12} \cdot \left(\frac{I_1}{I_2} \right) - \frac{\tan \phi_1}{2} \cdot \frac{S^2}{N_E^2} \cdot \frac{\sin^2 A_{12}}{I_2} + \tan \phi_1 \cdot \left(\frac{J_1 - J_2}{I_2} \right) - \frac{S^3}{6N_E^3} \cdot \cos A_{12} \sin^2 A_{12} \cdot \left(1 + 3 \tan^2 \phi_1 \cdot \frac{J_2}{J_1} \right) \qquad (27).$$

It is now necessary to transfer from the equivalent sphere to the ellipsoid; i.e., the spherical distance $N_E d\phi$ must be converted into an ellipsoidal meridian section of equivalent length. Mathematically, the following must hold:

$$N_E \, d\phi_{sphere} = M_m \, d\phi_{ellipse} \qquad (28).$$

Before accomplishing this, it is to be remembered that N_E is the radius of the equivalent sphere at point P_2 and $M_m d\phi_{ellipse}$ best defines the meridional arc if M_m is evaluated at the midpoint of the arc, i.e., at the latitude $\phi_1 + \frac{1}{2}d\phi$. To get at this unknown point, it is necessary to determine the variation of M_m at P_1 and then to approach it by the application of the differential quantity $\frac{1}{2}\delta\phi$. To the first order this can be represented as:

$$M_m = M_1 + \frac{\partial M}{\partial \phi} \frac{\delta \phi}{2}.$$

But

$$M = a(1 - e^2 \sin^2 \phi)^{-3/2} \cdot (1 - e^2) = \frac{a(1 - e^2)}{W^{3/2}},$$

and hence

$$\frac{\partial M}{\partial \phi} = \frac{3M \cdot (e^2 \cdot \sin \phi \cdot \cos \phi)}{W^2}$$

which yields the following value M_m at the desired point:

$$M_m = M_1 \cdot \left(1 + \frac{3}{2W^2} \cdot (e^2 \cdot \sin \phi_1 \cdot \cos \phi_1) \cdot \delta\phi \right) \qquad (29)$$

or, in terms of $1/M_m$ after binomial expansion:

$$\frac{1}{M_m} = \frac{1}{M_1} \cdot \left(1 - \frac{3}{2W^2} (e^2 \cdot \sin \phi_1 \cdot \cos \phi_1) \cdot \delta\phi \right) \qquad (30).$$

Unfortunately the quantity $\delta\phi$ is the unknown and steps will have to be taken to overcome it. This can be achieved in an iterative manner as follows:

$$d\phi = \frac{S}{M_1}\cdot\cos A_{12}\,\frac{I_1}{I_2} - \frac{\tan\phi_1}{2}\,\frac{S^2}{N_1M_1}\,\frac{\sin^2A_{12}}{I_2} - \frac{S^3}{6N_1^2M_1}\cdot\cos A_{12}\cdot\sin^2A_{12}\cdot\left(1 + 3\tan^2\phi_1\,\frac{J_2}{I_2}\right) +$$

$$\frac{N_1}{M_1}\cdot\tan\phi_1\cdot\left(\frac{J_1 - J_2}{I_2}\right) - \frac{3}{2W_1^2}\cdot\left(e^2\cdot\sin\phi_1\cdot\cos\phi_1\right)\cdot\delta\phi^2 \qquad (31),$$

where

$$\delta\phi = \frac{S}{N}\cdot\cos A_{12}\cdot\frac{I_1}{I_2} - \frac{\tan\phi_1}{2}\cdot\frac{S^2}{N_1^2}\cdot\frac{\sin^2A_{12}}{I_2} - \frac{S^3}{6N_1^3}\cdot\cos A_{12}\cdot\sin^2A_{12}\cdot\left(1 + 3\tan^2\phi_1\cdot\frac{J_2}{I_2}\right) + \tan\phi_1\cdot\left(\frac{J_1 - J_2}{I_2}\right) \qquad (32).$$

The separation in longitude between P_1 and P_2 at the initial epoch must now be considered. Referring to figure 1:

$$d\lambda = \lambda_{P_2} - \lambda_{P1} = \lambda_2 + \dot\lambda_2\cdot\Delta t - \lambda_1 - \dot\lambda_1\cdot\Delta t = \lambda_2 - \lambda_1 + (\dot\lambda_2 - \dot\lambda_1)\cdot\Delta t = d\lambda + d\dot\lambda\cdot\Delta t \qquad (33).$$

Applying the sine rule to $\Delta - P_2 - P_1 -$ Pole the following relationship which implies an equivalent sphere to the ellipsoid at P_2, as well as the equivalence of spherical and ellipsoidal azimuths, is obtained:

$$\frac{\sin(d\lambda)}{\sin\left(\frac{S}{N_2}\right)} = \frac{\sin A_{12}}{\cos(\phi_2 + \dot\phi_2\cdot\Delta t)} \qquad (34).$$

Substitution of equation 33 into this and simplification after expansion will yield the following closed form which pre-supposes the solution of the latitude problem:

$$d\lambda + d\dot\lambda\cdot\Delta t = \arcsin\left(\sin\left(\frac{S}{N_2}\right)\frac{\sin A_{12}}{\cos(\phi_2 + \dot\phi_2\cdot\Delta t)}\right) \qquad (35).$$

It may be convenient, although unnecessary at this stage, to expand equation 35 by a power series formula.

Finally the back azimuth must be computed. The technique for the determination is similar to that developed for latitude and longitude, in that equivalent spheres are used. Also the solution is dependent on a knowledge of $d\phi$ and $d\lambda$ and since it is assumed that $\dot\phi_i$ and $\dot\lambda_i$ are known, the method can be used for a wide variety of back azimuths in addition to the back azimuth of the observed section.

Referring to figure 3, the following cyclic spherical relationships are formed:

$$\frac{\tan\frac{1}{2}(a + b)}{\tan\frac{1}{2}c} = \frac{\cos\frac{1}{2}(A - B)}{\cos\frac{1}{2}(A + B)} \quad ; \text{ and } \quad \frac{\tan\frac{1}{2}(A + B)}{\cot\frac{1}{2}c} = \frac{\cos\frac{1}{2}(a - b)}{\cos\frac{1}{2}(a + b)} \qquad (36).$$

Substitution of the necessary parameters takes place, usually into equation 36, together with the condition that:

$$\tfrac{1}{2}(A + B) = \tfrac{1}{2}(A_{12} + 360 - A_{21}) = \tfrac{1}{2}(A_{12} + 180 - A_{12} - dA),$$

where $dA = A_{21} - A_{12} - 180,$

i.e.,

$$\tan \tfrac{1}{2}(A + B) = \tan\left(90 - \frac{dA}{2}\right) = \cot\left(\frac{dA}{2}\right).$$

After manipulation and simplification, the following form, which may be subjected to power series expansions, results:

$$dA = 2 \arctan\left\{\frac{\sin[\frac{1}{2}(\phi_1 + \dot{\phi}_1 \cdot \Delta t + \phi_2 + \dot{\phi}_2 \cdot \Delta t)]}{\cos[\frac{1}{2}(\phi_1 + \dot{\phi}_1 \cdot \Delta t - \phi_2 - \dot{\phi}_2 \cdot \Delta t)]} \cdot \tan(d\lambda + d\dot{\lambda} \cdot \Delta t)\right\} \tag{37}.$$

4.2 The Inverse Geodetic Problem

The inverse geodetic problem by Puissant type equations cannot be stated in explicit terms. It is therefore necessary to approach the problem in an iterative manner involving much initial simplification.

Expand equation 35 by power series to yield:

$$d\lambda + d\dot{\lambda} \cdot \Delta t = \frac{S}{N_2} \cdot \sin A_{12} \cdot \sec(\phi_2 + \dot{\phi}_2 \cdot \Delta t) \cdot \left\{1 - \frac{S^2}{6N_2^2} \cdot \left[1 - \sin^2 A_{12} \cdot \sec^2(\phi_2 + \dot{\phi}_2 \cdot \Delta t)\right]\right\} \tag{38},$$

and degenerate this equation by use of the fact that $S^2/(6N_2^2) << 1$, of the order of 6×10^{-5} for a 50 km line, into

$$S \sin A_{12} = (d\lambda + d\dot{\lambda} \cdot \Delta t) \cdot \cos(\phi_2 + \dot{\phi}_2 \cdot \Delta t) \cdot N_2 \tag{39}.$$

Consider now equation 32 which can also be degenerated by approximation into:

$$d\phi = \frac{S}{M_1} \cdot \cos A_n \cdot \frac{I_1}{I_2} \tag{40}.$$

Substitution of this first order equation into equation 39 yields:

$$\tan A_{12} = \frac{(d\lambda + d\dot{\lambda} \cdot \Delta t)}{d\phi} \cdot \frac{I_1}{I_2} \cdot \frac{N_2}{M_1} \cos(\phi_2 + \dot{\phi}_2 \cdot \Delta t).$$

S may now be determined from either equation 39 or equation 40. Using these values of S and A_{12}, an updated value of $S \cdot \sin A_{12}$ is computed from equation 38, and similarly $S \cdot \cos A_{12}$ from equation 31. The procedure is cycled until sufficient accuracy is obtained, oscillating between the alternative equations for efficiency of convergence.

The final quantity A_{21} is directly determined from a knowledge of dA as outlined in the direct geodetic problem.

4.3 General Remarks on the Geodetic Model

The equations and methods developed in this section are far from satisfactory for incorporation into an adjustment scheme as it is a non-trivial matter to obtain the partial derivatives or to form observation equations directly. A number of alternatives exist, not the least of which is the desirability of using equations other than the Puissant type. The developments of such forms is not

within the scope of this paper.

5. Summary

In summary it has been shown that it is possible to derive geodetic/photogrammetric models to determine a velocity field from observations of moving stations over a suitable time scale. KAULA (1973) has performed similar derivations and simulations for lunar laser ranging which will account for global plate tectonics while the geodetic model is expected to cover individual plate boundaries and other macro areas and the photogrammetric method could be expected to cover meso areas such as glaciers and volcanic regions.

The principal advantages of the velocity concept can be summarized as follows:

1) It provides rigorous derivations of the forces, stresses and strains that an area is undergoing. In particular, the yield point can be approached without fear of model breakdown.

2) Few surveys, except for pure photogrammetric cases, can be accomplished in time scales which are sufficiently short that all observations can be regarded as occurring at a standard epoch.

3) The passage of stress waves through a spatial field can be modelled by incorporating time into the velocity function active at the point.

4) In a secular environment where there are no fixed points available, the velocity approach allows a single centre of mass point of the array to be chosen and all data to be made relative to this point.

The principal disadvantage of the system is the increased complexity of the mathematical models associated with the deformations.

National Mapping has only this last field season begun surveys of which the principal aim has been the detection of crustal movement, although in certain instances the Australian Geodetic Datum can be used as a benchmark for future work. This traverse work, in conjunction with the high precision satellite and lunar programs, has necessitated that theoretical investigations into the most efficient and best data analysis methods for elucidating geophysical information from geodetic observations, be undertaken. In this regard, all the above developments have been checked against static cases for correctness.

Work is continuing on deriving simpler equations to handle the velocity concept and, where practical, of incorporating extra-terrestrial data into the model for its added strength at the macro level.

6. Acknowledgments

Many people have contributed to the ideas expressed in this paper. However, Mr. J. McK. Luck has been especially helpful in providing a most useful sounding board and in organizing the final production.

7. Notation

The following notations have been used.

7.1 Section 2

$X_p = \begin{pmatrix} x \\ y \\ z \end{pmatrix}_p$ a vector of space rectangular geocentric co-ordinates. In particular it usually applies to the co-ordinates of the point at the initial epoch

$X_1 = \begin{pmatrix} x \\ y \\ z \end{pmatrix}_p$ the same, but at epoch $t \neq 0$, i.e., at some epoch other than the initial epoch

$h_i(X_p)$ function of spatial co-ordinates

$h_i(t)$ velocity function with respect to time

η strain tensor

F three-dimensional vector of rectangular forces

A vector of face areas of a body being subjected to general three-dimensional forces

J the Jacobian

T stress tensor

$\dot{\eta}$ strain rate tensor

7.2 Section 3

x_p, y_p observed plate co-ordinates relative to the fiducial centre

x_o, y_o the calibrated values of the optical centre relative to the fiducial centre

f calibrated focal length

X_p a vector of ground station co-ordinates in a Cartesian rectangular system

X_o a vector of camera station co-ordinates in the co-ordinate system of X_p

$M = \begin{pmatrix} M_1 \\ M_2 \\ M_3 \end{pmatrix}$ the general rotation matrix ω, ϕ, χ

$V_p(t)$ a vector of velocity function not embodying X_p in any functional relationship

F, G, H general matrix functions

L_a the adjusted or true observations

L_b the observations to be adjusted

X_a the adjusted/true parameters

A $\partial F / \partial X_a$

B $\partial F / \partial L_a$

$P = \Sigma^{-1}$ a weight matrix of observations

X a vector of unknown parameters

X_o a vector of approximations to unknown parameters

K_i a vector of Lagrangian multipliers

W_i $F(L_b, X_o)$

7.3 Section 4

$\phi_i, \lambda_i, A_{ij}$ geodetic latitude, longitude and azimuth

$\dot{\phi}_i, \dot{\lambda}_i$ time rate of change of ϕ_i and λ_i

S	arc length - normal section
t	time
Δt	time interval
F,G	general matrix functions
(Δ - P_1- P_2- Pole)	the triangle with vertices P_1, P_2,Pole
M	the meridional radius of curvature of the ellipsoid
N	the prime vertical radius of curvature of the ellipsoid

8. References

BORG, S.F. 1963. *Matrix - Tensor Methods in Continuum Mechanics.* Van Nostrand,Princeton NJ.

BROWN, D.C. RCA54. Results in Geodetic Photogrammetry 1, The Precise Determination of the Location of Bermuda from Photogrammetric Observations of Flares Ejected from Juno II. *Rep.* 54, Radio Corporation of America.

BROWN, D.C. ET AL 1964. *Research in Mathematical Targeting, Volumes I,II & III.* Reports perpared for Rome Air Development Center, Griffiths Air Force Base, New York, under contract AF 30(602)-3007.

CLARK, D. 1963. *Plane and Geodetic Surveying,Volumes I & II.* (5th ed) Constable,London.

KAULA, W.M. 1973. Potentialities of Lunar Laser Ranging for Measuring Tectonic Motions. *Phil.Trans. R.Soc.Lond.A* 274,185-193.

LOVE, A.E.H. 1920. *A Treatise on the Mathematical Theory of Elasticity.* (3rd ed) Cambridge University Press.

SOKOLNIKOFF, I.S. 1956. *Mathematical Theory of Elasticity.* (2nd ed) McGraw-Hill,New York.

TIMOSHENKO, S. & GOODIER, J.N. 1951. *Theory of Elasticity.* (2nd ed) McGraw-Hill,New York.

UOTILA, U.A. 1967. *Introduction to Adjustment Computations with Matrices.* (Unpublished Lecture Notes) Department of Geodetic Science,The Ohio State University,Columbus Ohio.